

## Response to Short Comment

Comments are in black and responses are in blue.

We note that you define the entrainment and non-entrainment zone as the regions within 20-m above and below the height of maximum LWC in the VOCALS Sc, respectively; and you use these for describing the behavior of the droplet spectra and aerosol in the two zones. We also have been involved in an aircraft Sc field study (POST; 2008 off the CA coast) using the CIRPAS Twin Otter. The VOCALS and POST Sc should be quite similar given solid cloud cover and large temperature jumps above cloud top for both studies. Thus, it is of interest to do some initial comparisons here related to your comments on “entrainment in stratocumulus.”

You suggest dry and warm air entrained in VOCALS Sc dilutes Nd and LWC but leaves droplet sizes relatively unaffected, thus resembling extreme inhomogeneous entrainment/mixing. Also, you note that it is still unclear whether inhomogeneous or homogeneous mixing dominates, and that previous studies favor inhomogeneous mixing.

These suggestions are not far from what we found for the entrainment-mixing process in POST Sc; however, there are differences resulting from our look at the POST Sc using a different approach. We use a different vertical description in characterizing the region near Sc top (see Malinowski et al., 2013): “Cloud top” is defined as the maximum height of unbroken cloud. And above this cloud top the turbulent EIL (entrainment interface layer) extends up to the unaffected free atmosphere. Part of the EIL contains cloud filaments that are evaporating and where mixing can be termed extreme inhomogeneous. Cloud and sensible heat detraining from cloud top are key in reducing buoyancy in the EIL. Radiative cooling is centered at cloud top causing the generation of negative buoyancy.

Then, what is entrained into the unbroken Sc below our cloud top, is it homogeneous or inhomogeneous? An answer is suggested by Fig. 1 which shows a 2-s (~100 m) data sample of LWC and Re (effective radius) collected on POST flight TO6.

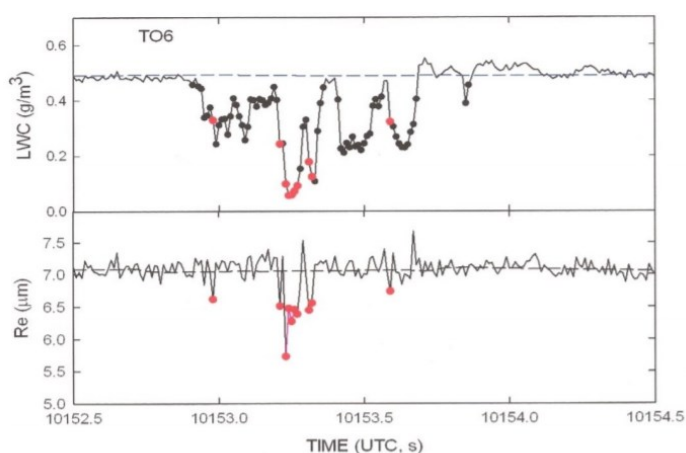


Fig. 1 – LWC and Re (effective radius) 20-cm horizontal resolution Sc data collected just below cloud top from POST flight TO6. Data points indicate the location of a descending entrained cloud parcel. The red data points indicate where both LWC and Re have decreased.

The LWC and Re data records in Fig. 1 both show relatively unchanging background values except for the location of the entrained parcel. Some Re values (red) show reduced values from the background indicating a change in the droplet size distribution and the probable presence of homogeneous mixing. However, most data points (black) only show a decrease in LWC. That sure looks again like extreme inhomogeneous mixing, but the black data more likely show a simple dilution of the cloud by air that has nearly the same buoyancy and moisture as cloud top, and that also preserves the value of Re. Gerber et al. (2016) give more details to support this conclusion including showing the independence of temperature reduction in entrained parcels from reduced LWC in the parcels (see Fig. 5 in that paper), and showing similar behavior of POST Sc with and without predicted buoyancy reversal using mixing fraction analysis.

Thus entrainment/mixing for the POST Sc, and likely also for the VOCALS Sc, is not simply extreme inhomogeneous mixing with warmer and dryer air causing the reduction of LWC and Nd in the Sc, but is a bit more complex with both extreme inhomogeneous mixing and homogenous mixing playing a role in the entrainment process. Yes, air entrained through Sc cloud top can change the droplet size spectrum as Fig. 1 suggests by the reduction of Re, but that appears secondary in most POST Sc in comparison to the dilution process that preserves the relative shape of the spectrum.

It would be interesting to know how your choice of entrainment and non-entrainment zones apply to the vertical-layer partitioning according to Malinowski et al. (2013), including your findings about droplet spectra and aerosol.

We thank Dr. Hermann Gerber very much for commenting on this manuscript. Please see the following detailed responses.

According to the method in Malinowski et al. (2013), the profile during 18<sup>th</sup> Oct was divided into four vertical layers (Fig. 1R), including the cloud-top layer (CTL), cloud-top mixing sublayer (CTMSL) and turbulent inversion sublayer (TISL), and free troposphere (FT). In our study, “cloud top” corresponds to the division between the TISL and CTMSL, and the division between non-entrainment and entrainment zone (the height of maximum LWC) is close to that between the CTL and CTMSL.

As Dr. Hermann Gerber pointed out, it is of interest to do some initial comparisons between the VOCALS and POST Sc due to the similar cloud properties and meteorological condition. Thus, we attempt to conduct a similar analysis to Fig. 1 in comments, but we are not able to capture as many “LWC holes” as in their study because of the relatively low temporal resolution in VOCALS cloud data (1Hz). Only two LWC holes are identified, and both are accompanied by simultaneous reduction of Re and Nd, which might indicate that both extreme inhomogeneous mixing and homogenous mixing playing a role in the entrainment process as described in Gerber et al. (2016). However, it is interesting that, in CTL, each reduction in LWC corresponds to a significant decrease in vertical velocity (Fig. R1f). Thus, another possibility is that, the decrease in LWC in CTL, may be due to evaporation of cloud droplets caused by the downdraft in the cloud instead of the entrained dry air.

Unfortunately, the data with relatively low temporal resolution prevent further exploration of

entrainment mixing in CTL as Dr. Hermann Gerber did. In our study, the entrainment and non-entrainment zone are defined as the regions within 20-m above and below the height of maximum LWC, respectively. As shown in Fig. R1c, there is no LWC hole identified in non-entrainment zone, and LWC is close to its adiabatic value. Given that the two zones are both thin layers, there is little difference in the dynamical and thermos-dynamical conditions. It is therefore assumed that the difference of cloud microphysical characteristics between the two zones is only caused by entrainment. Then, the difference of cloud microphysics between entrainment and non-entrainment zone are analyzed. That is, our study focused on the entrainment mixing in cloud-top mixing sublayer (CTMSL) rather than the cloud-top layer (CTL). As Dr. Hermann Gerber mentioned, in part of the EIL, mixing can be termed extreme inhomogeneous, which is consistent with our conclusion.

We acknowledge that it is still necessary to investigate the entrainment-mixing mechanism in CTL, although the entrainment in CTL might be weaker than that in CTMSL. However, in this study, the cloud data at a frequency of 1 Hz limit the further exploration of entrainment mixing in CTL. We are grateful for the important references provided by the Dr. Hermann Gerber, which have been cited in the revised manuscript to enhance the discussion of the entrainment-mixing mechanism in stratocumulus:

*Gerber, H., Malinowski, S. P., and Jonsson, H.: Evaporative and radiative cooling in POST stratocumulus, J. Atmos. Sci., 73, 3877– 3884, <https://doi.org/10.1175/Jas-D-16-0023.1>, 2016.*

*Malinowski, S. P., Gerber, H., Jen-La Plante, I., Kopec, M. K., Kumala, W., Nurowska, K., Chuang, P. Y., Khelif, D., and Haman, K. E.: Physics of Stratocumulus Top (POST): turbulent mixing across capping inversion, Atmos. Chem. Phys., 13, 12171-12186, <https://doi.org/10.5194/acp-13-12171-2013>, 2013.*

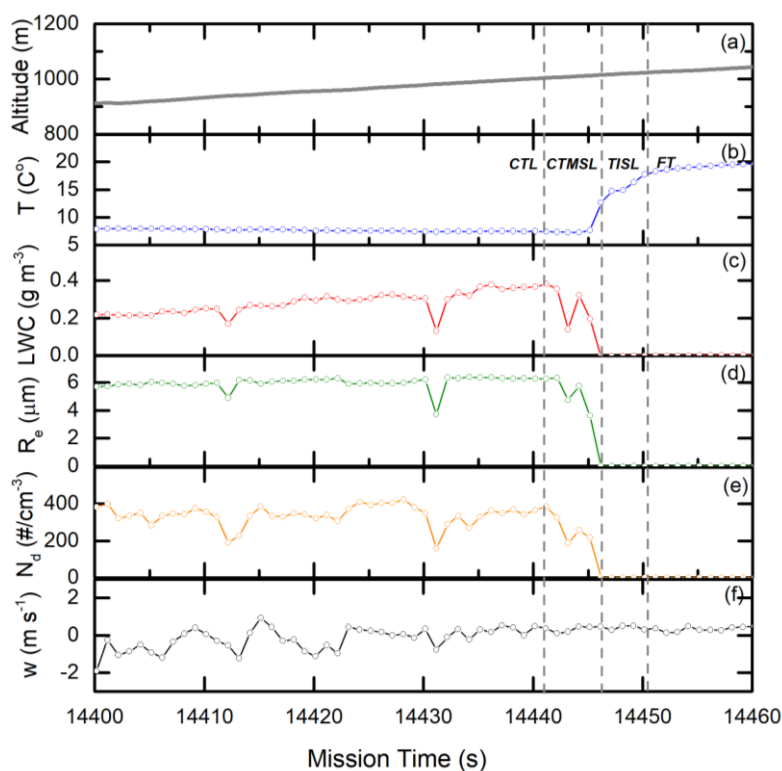


Fig. R1. The ascent of the aircraft for flight during 18<sup>th</sup> Oct showing 1-Hz (a) altitudes, (b)

temperature ( $^{\circ}\text{C}$ ), (c) LWC, (d)  $R_e$ , (e)  $N_d$ , and (f) vertical velocities as a function of time. The vertical dashed lines indicate the division of sublayers discussed in the text.

# Exploring aerosol cloud interaction using VOCALS-REx aircraft measurements

Hailing Jia<sup>1</sup>, Xiaoyan Ma<sup>1</sup> and Yangang Liu<sup>2</sup>

<sup>1</sup>Key Laboratory of Meteorological Disaster, Ministry of Education (KLME)/Joint International Research Laboratory of Climate and Environment Change (ILCEC)/Collaborative Innovation Center on Forecast and Evaluation of Meteorological Disasters (CIC-FEMD)/Key Laboratory for Aerosol-Cloud-Precipitation of China Meteorological Administration, Nanjing University of Information Science & Technology, Nanjing 210044, China

<sup>2</sup>Environmental and Climate Sciences Department, Brookhaven National Laboratory, Upton, NY, USA

Correspondence to: Xiaoyan Ma (xma@nuist.edu.cn)

**Abstract.** In situ aircraft measurements during the VAMOS Ocean-Cloud-Atmosphere-Land Study-Regional Experiment (VOCALS-REx) field campaign are employed to study the interaction between aerosol and stratocumulus over the southeast Pacific Ocean, as well as entrainment process near the top of stratocumulus and its possible impacts on aerosol-cloud interaction. Our analysis suggest that the increase of liquid water content ( $LWC$ ) is mainly ~~controlled~~~~contributed~~ by cloud droplet number concentration ( $N_d$ ) instead of effective radius of cloud droplets in the polluted case, in which more droplets form with smaller size, while the opposite is true in the clean case. By looking into the influences of dynamical conditions and aerosol microphysical properties on the cloud droplet formation, it is confirmed that cloud droplets are more easily to form under the conditions with large vertical velocity and aerosol size. An increase in aerosol concentration tends to increase both  $N_d$  and relative dispersion ( $\epsilon$ ), while an increase in vertical velocity ( $w$ ) often increases  $N_d$  but decreases  $\epsilon$ . After constraining the differences of cloud dynamics, positive correlation between  $\epsilon$  and  $N_d$  become stronger, implying that perturbations of  $w$  could weaken the influence of aerosol on  $\epsilon$ , and hence may result in an underestimation of aerosol dispersion effect. The difference of cloud microphysical properties between entrainment and non-entrainment zones ~~confirms~~~~suggests~~ that the entrainment-mixing mechanism is predominantly extreme inhomogeneous in the stratocumulus that capped by a sharp inversion, namely the entrainment reduces  $N_d$  and  $LWC$  by 28.9 % and 24.8 % on average, respectively, while the size of droplets is relatively unaffected. In entrainment zone, ~~smaller aerosols and~~ drier air entrained from the top induce less cloud droplet with respect to total in-cloud particles ( $0.56 \pm 0.22$ ) than the case in non-entrainment zone ( $0.73 \pm 0.13$ ) by ~~inhibiting aerosol activation and~~ promoting cloud droplets evaporation.

## 1 Introduction

Stratocumulus plays a key role in the radiative energy budget of the Earth by reflecting incoming shortwave radiation and thus cools the surface of the planet and offsets the warming by greenhouse gases (Hartmann et al., 1992). Stratocumulus clouds

30 are susceptible to aerosols, i.e. aerosol indirect effect (Twomey, 1974; Albrecht, 1989), which currently remains large uncertainties (Lohmann and Feichter, 2005; Chen and Penner, 2005; Carslaw et al., 2013; McCoy et al., 2017).

The marine stratocumulus overlaying the southeast Pacific Ocean (SEP) is the largest and most persistent clouds in the world (Klein and Hartmann, 1993; Bretherton et al., 2004). Sources of anthropogenic aerosol from the Chilean and Peruvian coasts, in contrast with relatively clean air masses from the Pacific Ocean, make the SEP an ideal region to explore the  
35 interaction of aerosol and stratocumulus cloud topped boundary layers. The cloud properties from satellite retrievals exhibit a gradient off the shore of Northern Chile. For example, cloud droplet number concentration decreased from 160 to 40  $\text{cm}^{-3}$  (George and Wood, 2010) and cloud droplet effective radius increased from 8 to 14  $\mu\text{m}$  from the coast to about 1000 km offshore (Wood et al., 2006). This gradient is plausibly ~~attributable~~ attributed to anthropogenic aerosol near the coast. Huneeus et al. (2006) found that during easterly wind events, sulfate increased one order of magnitude over SEP, which results in 1.6 to  
40 2 fold increase in cloud droplet number concentration. Based on observations from satellites and cruises, Wood et al. (2008) suggested that open cellular convection within overcast stratocumulus is associated with reduced aerosol concentration, and an air mass not passing through the Chilean coast, which further confirms the impact of aerosol on stratocumulus over SEP. However, it is difficult to establish the generality of previous studies based on satellite remote sensing due to the absence of in situ observations that provide vertical profiles of cloud and aerosol and detailed in-cloud processes.

45 The VAMOS (Variability of the American Monsoons) Ocean-Cloud-Atmosphere-Land Study-Regional Experiment (VOCALS-REx), which includes multiple aircraft missions, ship and land-based measurements, took place in the region extending from the near-coastal of northern Chile and southern Peru to the remote ocean in the SE Pacific during October–November 2008 (Wood et al., 2011). Studies based on this field campaign provided more information about the properties of aerosol, cloud and marine boundary layer over SEP. For instance, the multi-platform observations during VOCALS revealed  
50 that the boundary layer was shallow and fairly well mixed near shore but deeper and decoupled offshore (Bretherton et al., 2010). Twohy et al. (2013) found that higher aerosol concentrations near shore were associated with more but smaller cloud droplets, less liquid water path (*LWP*), and thus attributed to a combined effect of anthropogenic aerosol and the physically thinner clouds near shore. Nevertheless, an increase in *LWP* with the cloud condensation nuclei (CCN) concentrations was found during the similar meteorological conditions (Zheng et al., 2010). Additionally, chemical components and sources of  
55 aerosols during VOCALS-REx campaign have been discussed in several studies (Chand et al., 2010; Hawkins et al., 2010; Allen et al., 2011; Twohy et al., 2013; Lee et al., 2014). Although these studies improved our understanding of aerosol, cloud and boundary layer properties over SEP, the mechanisms of the detailed processes on interaction between aerosol and stratocumulus cloud is still unclear.

By employing in situ aircraft data collected by CIRPAS Twin Otter aircraft during VOCALS-REx, we investigate the  
60 following issues in this study: (a) the relationships between aerosol and cloud properties; (b) cloud droplet formation and its

influencing factors; (c) dispersion effect (i.e., the influence of aerosol on the shape of cloud droplet size spectrum), and (d) entrainment process near the top of stratocumulus and its impact on cloud. This paper is organized as follows: The instruments and measurement data are described in Sect. 2, and the main results are discussed in Sect. 3. A summary and discussion is given in Sect. 4.

## 65 2 Data and method

### 2.1 Aircraft Data

The Twin Otter operated by the Center for Interdisciplinary Remotely Piloted Aircraft Studies (CIRPAS) was aimed to observe aerosol, cloud microphysics, and turbulence near Point Alpha (20° S, 72° W) off the coast of Northern Chile from 16 October to 13 November 2008. A total of 19 flights were carried out, each of which conducting about 3 hours of sampling at Point Alpha and including several soundings and horizontal legs near the ocean surface, below the cloud, near the cloud base, within the cloud, near the cloud top, and above the cloud (Fig. 1). Since all flight tracks are similar, only one track (Oct. 18) is shown in Fig. 1. As cloud and aerosol probe measurements failed during the flight on 5 November and drizzle processes occurred on the flights on 1 November and 2 November, only the observations from other 16 non-drizzling flights are included in this paper.

75 ~~Both the aerosol below and above clouds and the interstitial aerosol in-cloud data was were~~ obtained by Passive Cavity Aerosol Spectrometer Probe (PCASP-100), which counted and sized particles from 0.1–2.0  $\mu\text{m}$  dry diameter with 20 bins (Zheng et al., 2011; Cai et al., 2013; Twohy et al., 2013). The CCN number concentration was observed by the CCN Spectrometer at a supersaturation of 0.2 % and 0.5% respectively. The cloud data include cloud droplet number concentration ( $N_d$ , size range: 2.07–40.2  $\mu\text{m}$  with 20 bins) from the Cloud, Aerosol and Precipitation probe (CAS), effective radius of cloud droplets ( $R_e$ ), and liquid water content ( $LWC$ ) from the PVM-100 probe (Gerber et al., 1994). All data sets used in this study are at a frequency of 1 Hz. The calibrations of the onboard instruments were carried out so as to provide standard meteorological variables, aerosol, and cloud observations. Zheng et al. (2011) pointed out that uncertainties of aerosols and cloud measured by these probes are within 15 %. More detailed information about the observation instruments on board the CIRPAS Twin Otter aircraft during VOCALS-REx can be found in Zheng et al. (2010) and Wood et al. (2011).

### 85 2.2 Data processing

In this study, the data collected near the land, during both take-off and landing, are removed to ensure only the measurements close to Point Alpha (20° S, 72° W) are analysed. The occurrence of clouds is defined by the following criterion, i.e.,  $LWC > 0.05 \text{ g m}^{-3}$  and  $N_d > 15 \text{ cm}^{-3}$ . We averaged the CCN number concentrations during the legs within 200 m above the cloud top to obtain the average above-cloud CCN, and within 200 m below the cloud base to obtain the mean sub-cloud CCN.

90 During the study period, the CCN Spectrometer constantly measured CCN at a supersaturation of 0.2 % except on the first four flights at a supersaturation of 0.5 %. In order to have a consistent comparison between all flights, we adopted the method by Zheng et al. (2011) to adjust the CCN concentration from supersaturation of 0.5 % to 0.2 % on the first four flights. Since the effective diameter of aerosol particle is not measured directly, so we calculated it according to the measurements of aerosol size distribution based on following equation:

$$95 \quad Da = \sum n_i d_i^3 / \sum n_i d_i^2 \quad (1)$$

where  $n_i$  is the aerosol number concentration in the  $i$ th bin of PCASP, and  $d_i$  represents the arithmetic mean diameter of  $i$ th bin.

To investigate the impact of the entrainment process on cloud properties and aerosol-cloud interaction, we defined entrainment zone and non-entrainment zone, respectively. Gerber et al. (2005) showed that, in the marine stratocumulus, entrainment occurs when  $LWC$  begins to decrease from the bottom of the cloud. In this manuscript, entrainment and non-entrainment zone are thus defined as the regions within 20 m above and below the height of maximal  $LWC$ , respectively. 100 Given that the two zones are both thin layers, there is little difference in the dynamical and thermos-dynamical conditions. It is therefore assumed that the difference of cloud microphysical characteristics between the two zones is only caused by entrainment.

### 3 Results

#### 105 3.1 Vertical profiles of aerosol, cloud and meteorological variables

The vertical profiles of aerosol, cloud and meteorological variables during 16 flights are scaled by the inversion height ( $z_i$ ) (Fig. 2), which is defined as the height where the vertical gradient of liquid water potential temperature ( $\theta_L$ ) is the largest (Zheng et al, 2011).  $\theta_L$  is conservative for water phase changes, but same as potential temperature when no liquid water exist (Betts, 1973). This normalization could exclude the variation of  $z_i$  between flights, and hence better for exploring the average BL structure during VOCALS-REx. 110

As shown in Fig. 2a, temperature ( $T$ ) decreases sharply with the height within the BL, which is close to dry adiabatic lapse rate. A strong inversion occurs at the top of the BL, with the average temperature change about 10 °C. Due to reduced  $T$  and nearly constant water vapor mixing ratio within strong mixing BL, relative humidity ( $RH$ ) increases rapidly with the height (Fig. 2b).  $T$  and  $RH$  reach the minimum and maximum, respectively, when  $z/z_i$  is close to 0.9. Near the top of the BL ( $0.9 < z/z_i < 1.0$ ), the entrainment of the dry and warm air from the free atmosphere aloft results in a slight increase in  $T$  and a slight decrease in  $RH$ . When  $z/z_i > 1$ ,  $T$  increases to about 18 °C and  $RH$  decreased to about 16 % rapidly (Fig. 2a, b). The vertical profiles of  $T$  and  $RH$  are overall consistent with the observations of other marine stratocumulus clouds (Martinet et al., 1994; Keil and Haywood, 2003). ~~Corresponding to vertical variation of  $RH$ , the  $N_a$  gradually increases with the height, reaches the maximum when  $RH$  is maximum ( $z/z_i = 0.9$ ), and then decreases when  $0.9 < z/z_i < 1.0$ , indicating that more cloud droplets are~~

120 nucleated in high supersaturation. The profile of  $LWC$  and  $R_e$  is similar to that of  $N_d$  (Fig. 2d, e). For cloud properties, an  
average of all profiles that normalized by  $z_i$  only may be insufficient to indicate the vertical variation of clouds, due to the  
different cloud base height of each profile. Thus, the average profiles are not shown in Fig. 2c, d, e, and the vertical variation of  
cloud properties can be seen easily from the single profile. Corresponding to vertical variation of  $RH$ , the  $LWC$  gradually  
increases with the height, reaches the maximum when  $RH$  is maximum ( $z/z_i = 0.9$ ), and then decreases when  $0.9 < z/z_i < 1.0$ .  
125 The profile of  $R_e$  is similar to that of  $LWC$  (Fig. 2e). For  $N_d$ , the green profile remains relatively constant, and the red one shows  
a slight increase with height. In general, the  $N_d$  profile remains relatively constant with a slight increase and decrease near base  
and top, respectively (Fig. S1), which is consistent with results in other VOCALS-REx observations (Painemal and Zuidema,  
2011). Fig. 2f reveals that the effective diameter of aerosol particles ( $D_a$ ) below cloud is larger than that above cloud, which is  
probably ~~attributable~~ attributed to the different chemical composition and sources of aerosols. The profile of  $CCN/CN$  is similar  
130 to that of  $D_a$  (Fig. 2g), suggesting that aerosols with large size are more likely to become CCN (Dusek et al., 2006; Zhang et al.,  
2011). Larger  $D_a$  and  $CCN/CN$  are also found in polluted case than clean cases.

### 3.2 Relationships between aerosol and cloud properties

Aerosol indirect effect is one of the largest uncertainties in current climate assessments. Most studies based on satellite  
data employed aerosol optical depth or aerosol index as agents of CCN number concentration to investigate the aerosol-cloud  
135 interactions (Koren et al., 2005, 2010; Su et al., 2010; Tang et al., 2014; Ma et al., 2014, 2018; Wang et al., 2014, 2015;  
Saponaro et al., 2017). However, not all aerosols ~~on-in~~ in the vertical column are actually involved in cloud formation, thus this  
assumption is relatively rough. Several studies revealed that aerosols have little effect on cloud properties when aerosol and  
cloud layers are clearly separated (Costantino and Bréon, 2010, 2013; Liu et al., 2017). In this study, the impact of CCN  
number concentration near cloud layer, e.g. below and above cloud respectively, on cloud properties is assessed.

140 The relationships between sub-cloud CCN number concentration ( $sub-CCN$ ) and cloud properties during all flights are  
shown in Fig. 3. The red dots signify the ten flights with typical well mixed boundary layer and non-drizzling cases, which  
have relatively similar meteorological conditions, such as similar inversion heights, and the jump of potential temperature and  
total water mixing ratio across the inversion (Zheng et al., 2010), and thus can be used to isolate the response of cloud  
properties to aerosol perturbations. The blue dots represent the other cases, in which the conditions except typical well mixed  
145 boundary layer and non-drizzling, such as strong wind shear within the BL, moist layers above clouds, strong decoupled BL  
and so on, are involved (Table 2). In the case of typical well mixed boundary with non-drizzling, both  $LWC$  (Fig. 3a) and  $N_d$   
(Fig. 3b) exhibit the positive relationships with  $sub-CCN$ , with correlation coefficients of 0.60 and 0.79, respectively, while  $R_e$   
has no evident correlation with  $sub-CCN$  (Fig. 3c). This may imply that the increase of  $LWC$  induced by  $sub-CCN$  is mainly  
caused by increasing  $N_d$  instead of  $R_e$ . Fig. 3d indicates a positive correlation between cloud depth and  $sub-CCN$ , with  
150 correlation coefficient of 0.71. As cloud top height is mainly determined by the temperature inversion condition, there is no

obvious correlation between cloud top height and sub-CCN, with correlation coefficient of only  $-0.13$  (Fig. 3e). However, the correlation coefficient between cloud base height and *sub-CCN* is  $-0.69$  (Fig. 3f), suggesting that CCN thickening cloud is mainly induced by lowering cloud base. It is noted that the above conclusions are only valid in the typical mixed boundary layer. In other cases (i.e. blue dots), the impacts of aerosols on the cloud is not evident due to large difference in the meteorological conditions and the boundary layer structure.

Compared to sub-cloud CCN, the influence of above-cloud CCN on cloud properties is very weak. The absolute values of correlation coefficient between above-cloud CCN number concentration (*abv-CCN*) and cloud properties are all less than 0.4 (~~not shown figure omitted~~), none of which pass the significance test ( $\alpha = 0.05$ ). In this study, above-cloud aerosol number concentration is very low ( $129.8 \pm 60.1 \text{ cm}^{-3}$ ) and the inversion capped the cloud top is extremely strong, which weakens the mixing of the aerosol with cloud layer and hence the effects of aerosol on cloud properties. Some previous studies based on aircraft observation for stratocumulus clouds also found that  $N_d$  exhibits a significantly positive correlation with *sub-CCN*, but no correlation with *abv-CCN* (Martin et al., 1994; Hudson et al., 2010; Hegg et al., 2012).

In order to investigate cloud formation in different aerosol loadings, the most polluted (Oct. 19) and the cleanest (Nov. 09) cases with aerosol concentrations of  $647.78 \pm 60.47 \text{ cm}^{-3}$  and  $268.97 \pm 35.67 \text{ cm}^{-3}$ , respectively, are selected in this study. Vertical profiles for the two cases are highlighted in Fig. 2, showing that  $N_d$  and  $LWC$  in polluted case are larger than those in clean one, but  $R_e$  remains the same. The low aerosol concentrations under the clean case inhibit the increase of  $N_d$  with  $LWC$  (Fig. 4a), which hence promotes the rapid increase of  $R_e$  with  $LWC$  (Fig. 4b). On the contrary, there are enough particles which may potentially activated into cloud droplets under the polluted case, thus  $N_d$  increases rapidly with  $LWC$ . ~~As the certain amount water is shared by large amount partieles,~~ However, due to a large number of aerosols competing for limited water vapor, the increase of  $R_e$  is ~~not significant~~ limited. It is suggested that the increase of  $LWC$  is mainly ~~controlled~~ contributed by  $N_d$  instead of  $R_e$  when aerosol concentrations is high, in which large number of cloud droplets are formed with smaller size, but the opposite is true when aerosol concentrations is low. The result is consistent with the study in Beijing by Zhang et al. (2011), but the difference of cloud formation between clean and polluted conditions is less evident, which is probably ~~attributable~~ attributed to the much lower aerosol concentration difference between clean and polluted cases in this study (about  $400 \text{ cm}^{-3}$ ) than that in Zhang et al. (2011) (about  $7000 \text{ cm}^{-3}$ ).

### 3.3 Cloud droplet formation and its controlling factors

Sub-cloud CCN is considered as a good proxy for the aerosol entering cloud. However, during actual flight, it is difficult to collect enough samples of sub-cloud CCN and cloud droplets simultaneously, which may result in uncertainty in statistical analysis. This limitation can be overcome by employing interstitial aerosols. Interstitial aerosols are particles observed in-cloud that either never activate into cloud droplets or have been activated but then return into aerosols after evaporation of cloud droplet. Kleinman et al. (2012) pointed out that the number concentration of interstitial aerosol ( $N_i$ ) can be obtained

either directly from the observation of in-cloud aerosols, or indirectly from a number balance between sub-cloud and in-cloud particles. In this study, the interstitial aerosol properties are derived from direct measurements in cloud. By employing aircraft observations over both land and ocean, Gultepe et al. (1996) found that the difference of the number concentration between total in-cloud particles ( $N_d + N_i$ ) measured directly and sub-cloud aerosols is very small. It is thus assumed that total in-cloud particles can characterize the overall level of in-cloud aerosol concentration before activation. The flight on Oct. 18 is singled out as a case study to support this assumption (Fig. 5). It is shown that the number concentrations of sub-cloud aerosols and total in-cloud particles are very close, with the values of  $583.7 \pm 55.4 \text{ cm}^{-3}$  and  $567.4 \pm 59.1 \text{ cm}^{-3}$  respectively. Similar results are also found in other flights. The average ratio of  $N_d + N_i$  to sub-cloud aerosol concentration during all flights is 0.94, which is much smaller than the value (1.29) found by Kleinman et al. (2012) based on G-1 aircraft during VOCALS-REx. Therefore, the observation of interstitial aerosols in this study is unlikely to be significantly interfered by factors such as cloud droplet shatter and cloud droplet evaporation due to instrument heating, as discussed by Kleinman et al. (2012), which has the potential to create ~~spurious~~more extra aerosols in-cloud.

The relations between  $N_d$  and  $N_d + N_i$  during 16 non-drizzling flights are shown in Fig. 6, in which the colors represent in-cloud vertical velocities. Positive correlations between  $N_d$  and  $N_d + N_i$  are found in all flights, representing the aerosol-cloud interaction (IPCC, 2001, 2007, 2013; Hegg et al., 2012). In addition, the effect of dynamical conditions on cloud droplet formation is evident. As presented in Fig. 6, data are close to the 1:1 line when vertical velocity is relatively large, namely in-cloud aerosols are almost entirely activated into cloud droplets. However, data deviate from the 1:1 line when vertical velocity is small or negative. For example, for all flights, the average ratio of  $N_d$  to  $N_d + N_i$  with vertical velocity greater than  $1 \text{ m s}^{-1}$  is  $0.84 \pm 0.12$ , which is much larger than that with vertical velocity less than  $-1 \text{ m s}^{-1}$  ( $0.64 \pm 0.14$ ). This is possibly ~~attributable~~attributed to high supersaturation caused by the adiabatic uplift under conditions with large vertical velocity. High supersaturation not only induces more aerosols to reach critical supersaturation and then activate into cloud droplets, but also inhibits cloud droplet evaporation.

In addition to dynamical conditions, aerosol microphysical properties, such as size distribution and chemical components, also affect activation process significantly (Nenes et al., 2002; Lance et al., 2004; Ervens et al., 2005; Dusek et al., 2006; McFiggans et al., 2006; Zhang et al., 2011; Almeida et al., 2014; Leck and Svensson, 2015). Since part of ~~aerosols~~aerosol population in the cloud have~~has~~ activated ~~to cloud droplets~~, it is difficult to obtain the information of aerosol size before activation. According to Köhler theory, the critical supersaturation of aerosol with large size is relatively low, and thus they activate preferentially, i.e. the effective diameter of interstitial aerosol ( $D_i$ ) is smaller than that of initial aerosols before activation. Li et al. (2011) compared the difference of size distribution between interstitial aerosol and aerosols that have been activated to cloud droplets, and found that the peak diameter of the former ( $0.45 \mu\text{m}$ ) was much smaller than that of the latter ( $0.8 \mu\text{m}$ ). It can be thus inferred that the size of aerosols activated to cloud droplets, and thus the size of initial aerosols would

be larger with the increase of  $D_i$ , though the quantitative relation depends on in-cloud dynamics. Therefore, it is assumed that, when compared with the data measured at different sampling locations during flight, the size of interstitial aerosol can still represent the size of initial aerosols before activation to some extent. As indicated in Fig. 7, the larger  $D_i$  is, the closer the data is to the 1:1 line, i.e. the higher proportion of cloud droplets in total in-cloud particles ( $N_d/(N_d + N_i)$ ) is. The averaged  $N_d/(N_d + N_i)$  for all flights is  $0.76 \pm 0.13$  when  $D_i$  is larger than  $1.0 \mu\text{m}$ , but only  $0.64 \pm 0.23$  when  $D_i$  is less than  $0.5 \mu\text{m}$ . It is because ~~that~~ those aerosols with large size are more likely to be activated into cloud droplets. Additionally, as larger aerosol particles form into larger cloud droplets (Twohy et al., 1989, 2013) that are relatively difficult to evaporate, large particles can also inhibit cloud droplet evaporation to a certain extent.

### 3.4 Dispersion effect

In addition to modulating the cloud droplet number concentration, aerosols also affect the shape of cloud droplet size spectrum (referred to as “dispersion effect”) and thereby cloud albedo (Liu and Daum, 2002). When the dispersion effect is taken into account, the estimated aerosol indirect forcing could be either reduced (Liu and Daum, 2002; Peng and Lohmann, 2003; Kumar et al., 2016; Pandithurai et al., 2012) or enhanced (Ma et al., 2010), i.e., dispersion effect could act to either offset or enhance the well-known Twomey effect, which mainly depends on the sensitivity of the relative dispersion ( $\varepsilon$ , the ratio of the standard deviation to the mean radius of the cloud droplet size distribution) on aerosol number concentration ( $N_d$ ). However, the relationship between  $\varepsilon$  and  $N_d$  still remains large uncertainty. Table 1 shows that the observed correlations between  $\varepsilon$  and  $N_d$  (or  $N_a$ ) can be positive, negative, or not evident. Different relations are indicative of the fact that the effect of aerosol on  $\varepsilon$  is often intertwined with effects of other factors, especially cloud dynamical conditions (Pawłowska et al., 2006; Lu et al., 2012). In this section, the relationship between  $\varepsilon$  and  $N_d$  based on the in-flight and the flight-averaged data are discussed respectively in order to distinguish the influences of aerosol and cloud dynamics on  $\varepsilon$ .

Within an individual flight, aerosol number concentration and chemical components can be assumed to be similar, providing an opportunity to focus on the effect of cloud dynamics to the extent possible. Here, we employ vertical velocity ( $w$ ,  $\text{m s}^{-1}$ ) as a proxy for cloud dynamical condition. As shown in Fig. 8, the correlations between  $\varepsilon$  and  $N_d$  based on in-flight data is significantly negative during all 16 non-drizzling flights, which is mainly modulated by  $w$ , i.e., larger  $w$  corresponds to a smaller  $\varepsilon$  but larger  $N_d$ . High supersaturation leads to more cloud droplets to activate and grow to the same size (i.e., narrow the droplet spectrum) when  $w$  is relative large, but a portion of cloud droplets may evaporate into smaller size and even deactivate into interstitial aerosols when  $w$  is small or even negative, resulting in the decrease of  $N_d$  and the broadening of the droplet spectrum.

It is interesting to see from Table 1 that the correlations between  $\varepsilon$  and  $N_d$  based on in-flight data are generally negative, while the one based on the flight-averaged data could be either positive, negative, or even uncorrelated. The uncertain relationships of the later may result from variations of the strength of cloud dynamic between flights, which would disrupt or

even cancel the real influence of aerosol on relative dispersion (Peng et al., 2007; Lu et al., 2012). However, many previous studies did not take the difference of cloud dynamics in flights into account when correlating  $\varepsilon$  and  $N_d$ , which could result in some degree of overestimation or underestimation of dispersion effect. In this study, data in all flights were sampled over the same location, i.e., Point Alpha, which can reduce the difference of dynamic conditions caused by variations of horizontal sampling location. In addition, we also distinguish the flights of typical mixed boundary layer and the others to ensure relatively similar meteorological conditions (see section 3.2). Fig. 9 shows the probability distribution function of  $w$  with mean values and standard deviations for 16 non-drizzling flights. The related statistics are shown in Table 2. It can be found that, except for other cases (~~gray shadow crosses~~; especially Oct. 24, Oct. 29, Nov. 8, and Nov. 13), the difference of in-cloud dynamics between typical well mixed boundary flights is very small, which confirms the assumption of similar meteorological conditions. As indicated in Fig. 10a,  $\varepsilon$  and  $N_d$  are positively correlated (correlation coefficient of 0.29 and the slope of  $1.9 \times 10^{-4}$ ) in the case of the typical well mixed boundary, indicating that aerosol increases  $\varepsilon$  and  $N_d$  at the same time. However, correlation coefficient and slope reduce to 0.11 and  $7.7 \times 10^{-5}$ , respectively in the all cases (i.e., not to constrain  $w$ ), implying that the influence of aerosol on  $\varepsilon$ - $N_d$  relationship tends to be weaker after intertwined with effects of cloud dynamics. Although the perturbations of cloud dynamics have been eliminated as far as possible,  $N_d$  is still likely determined by both aerosols number concentrations and updraft velocity together. Therefore, similar statistical analysis are also conducted for sub-cloud CCN. The relationship between  $\varepsilon$  and sub-cloud CCN is similar to that between  $\varepsilon$  and  $N_d$ , but, as expected, the correlation coefficient (slope) in the case of typical well mixed boundary and all cases increase to 0.67 ( $3.1 \times 10^{-4}$ ) and 0.31 ( $2.1 \times 10^{-4}$ ), respectively (Fig. 10b).

### 3.5 Entrainment in stratocumulus

Entrainment is a key process in the clouds, which plays an important role in the formation and evolution of clouds and the change of droplet spectrum, as well as aerosol indirect effect (Chen et al., 2014, 2015; Andersen and Cermak, 2015). The nature of entrainment is related to the cloud type. Entrainment in cumulus is primarily lateral with strong dilution of the cloud, which induces  $LWC$  to decrease rapidly to about 20% of its adiabatic value (Warner, 1955). Entrainment in stratocumulus is mainly determined by the strength of the gradients in buoyancy and horizontal winds (Wang and Albrecht 1994; Gerber et al. 2005; de Roode and Wang 2007; Wood, 2012), and proceeds from the top and affects mostly a thin layer (Gerber et al., 2005), whose dilution effect is much weaker than that in cumulus (Warner, 1955, 1969a, 1969b; Blyth et al., 1988; Gerber et al., 2008; Burnet and Brenguier, 2007; Haman et al., 2007). Aircraft observations of marine stratocumulus showed that the vertical profile of  $LWC$  is essentially same as the adiabatic profile, i.e. the cloud is almost adiabatic (Keil and Haywood, 2003).

In order to explore the entrainment in stratocumulus during VOCALS-REx, we firstly compared the differences of cloud microphysics between entrainment and non-entrainment zone near the cloud top. Here, entrainment and non-entrainment zone are defined as the regions within 20 m above and below the height of maximal  $LWC$ , respectively. As anticipated, adiabatic

275 fraction ( $AF$ , the ratio of the measured  $LWC$  to its adiabatic value) in entrainment zone ( $AF_{ent}$ ) is generally lower than that in  
non-entrainment zone ( $AF_{non-ent}$ ), with the mean values of all flights of 0.64 and 0.77 respectively (Table 2), which further  
confirms the rationality in dividing the two zones. Compared with non-entrainment zone, the peak diameters of cloud droplets  
in entrainment zone has little change (Fig. 11), and the effective diameters of cloud droplet ( $D_e$ ) increases only by 1.8 % (Table  
2). However,  $N_d$  and  $LWC$  decrease significantly by 28.9 % and 24.8% respectively on average (Table 2), especially during  
280 flights on Oct. 18, Nov. 04, Nov. 09 and Nov. 13,  $N_d$  decreases by 60.1 %, 56.3 %, 56.1 % and 59.2 %, and  $LWC$  decreases by  
55.7 %, 62.1 %, 55.8 % and 58.7 %, respectively (Table 2). It is suggested that dry and warm air entrained from cloud top  
dilutes  $N_d$  and  $LWC$  by a similar amount, while the size of droplets is relatively unaffected, which is thought as extreme  
inhomogeneous entrainment-mixing process. Moreover, both  $P_{LWC}$  and  $P_{N_d}$  are negatively correlated with  $AF_{ent}/AF_{non-ent}$ , with  
correlation coefficients of -0.60 and -0.47, respectively, indicating the dependence of the changes in  $LWC$  and  $N_d$  on the  
285 changes in adiabatic fraction (Fig. S2), where  $P_{LWC}$  and  $P_N$  are the percentages of reduction in  $LWC$  and  $N_d$  within entrainment  
zone relative to non-entrainment zone. Although it is still unclear whether the entrainment-mixing mechanism is  
predominantly homogeneous, inhomogeneous, or in between (Andrejczuk et al., 2009; Lehmann et al., 2009), Some  
previous studies showed that stratocumulus is, in general, dominated by the inhomogeneous (Pawlowska et al., 2000; Burnet  
and Brenguier, 2007; Haman et al., 2007; Lu et al., 2011; Yum et al., 2015). Furthermore, By employing a different vertical  
290 description in characterizing the region near cloud top (Malinowski et al., 2013), Gerber et al. (2016) pointed out that both  
extreme inhomogeneous mixing and homogenous mixing play a role in unbroken stratocumulus, but the reduction in cloud  
droplet effective radius appears secondary in comparison to the dilution process that preserves the relative shape of the droplet  
spectrum.

In this study, the flight on Oct. 18 with strong entrainment is chosen to investigate the difference of cloud droplet  
295 formation between entrainment and non-entrainment zone. As presented in Fig. 12b, dry and warm air entrained from the top  
reduces the relative humidity in entrainment zone by 8.8 % on average, and hence acts to accelerate the cloud droplets  
evaporation. As a consequence,  $N_d/(N_d + N_j)$  in entrainment zone ( $0.56 \pm 0.22$ ) is much lower than that in non-entrainment  
zone ( $0.73 \pm 0.13$ ) (Fig. 12c). Moreover, the relative dispersion in entrainment zone is overall larger than that in  
non-entrainment zone (Fig. 12d), implying that drier air entrained from the top could broaden cloud droplet spectrum by  
300 promoting the evaporation of cloud droplets. Some previous observations also showed that  $\varepsilon$  with low  $AF$  tends to be larger  
than that with high  $AF$ , and attributed it to the effect of entrainment mixing (Pawlowska et al., 2006; Lu et al., 2009). It is noted  
that the probability of  $D_i$  in entrainment zone is significantly higher than that in non-entrainment zone when  $D_i < 0.75 \mu\text{m}$ , but  
the opposite is true when  $D_i > 1.1 \mu\text{m}$  (Fig. 12a). This result suggests that, in addition to dry and warm air, small particles are  
also entrained into cloud from the top (Fig. 2f) and large particles are detrained out cloud at the same time. However, inversion  
305 capping a typical stratocumulus is usually too strong to excite significant updrafts near cloud top (Stevens, 2002; Wood, 2012;

Malinowski et al., 2013). Ghate et al. (2010) found that vertical velocities near the top of stratocumulus overall tend towards zero with only about 4% of updrafts stronger than  $0.5 \text{ m s}^{-1}$ . Therefore, although smaller aerosols are entrained into the entrainment zone, these aerosols seem unlikely to influence droplet formation by inhibiting activation due to the negligible cloud nucleation here. The effect of entrainment mixing on stratocumulus is mainly governed by the entrained dry air rather than small aerosols.

As shown in previous studies, nucleation of cloud droplet mainly occurs near cloud base, and sub-cloud aerosols are the major source of cloud droplets (Pinsky and Khain, 2002; Ghan et al., 2011). However, de Rooy et al., (2013) pointed out that entrainment mixing at the cloud edge and cloud top contribute significantly to the amount of entrained air and hence aerosols. Therefore, activation of aerosols is not restricted to the cloud base, where the central updraft enters the cloud (primary activation). Slawinska et al. (2012) found that a significant part (40%) of aerosols is activated above cloud base (secondary activation), which is dominated by entrained aerosols. By using large eddy simulations (LES), Hoffmann et al. (2015) suggested that, in a shallow cumulus, sub-cloud aerosols and laterally entrained aerosols contribute to all activated aerosols inside the cloud by fractions of 70% and 30%, respectively. Although entrainment in stratocumulus, discussed in this manuscript, is weaker than that in cumulus, entrained aerosols is still a possible source of cloud droplets. In this study, the flight on Oct. 18 with strong entrainment is chosen to investigate the difference of cloud droplet formation between entrainment and non-entrainment zone. As presented in Fig. 12a, the probability in entrainment zone is significantly higher than that in non-entrainment zone when  $D_i < 0.75 \mu\text{m}$ , but the opposite is true when  $D_i > 1.1 \mu\text{m}$ . This result indicates that small particles are entrained into cloud from the top (Fig. 2f) and large particles are detrained out cloud at the same time. The decrease of  $D_i$  by  $0.18 \mu\text{m}$  may inhibit aerosol activation into cloud droplet. Furthermore, dry and warm air entrained from the top reduces the relative humidity by 8.8% on average (Fig. 12b), and accelerates the cloud droplets evaporation. As a result,  $N_d / (N_d + N_i)$  in entrainment zone ( $0.56 \pm 0.22$ ) is much lower than that in non-entrainment zone ( $0.73 \pm 0.13$ ) (Fig. 12c). It is also noted that the relative dispersion in entrainment zone is overall larger than that in non-entrainment zone (Fig. 12d), implying that smaller aerosol particles and drier air entrained from the top could broaden cloud droplet spectrum by influencing nucleation and evaporation of cloud droplets. Some previous observations also showed that  $c$  with low  $AF$  tends to be larger than that with high  $AF$ , and attributed it to the effect of entrainment mixing (Pawlowska et al., 2006; Lu et al., 2009). According to the discussion in Sect. 3.3, although the impact of above cloud aerosol on whole cloud is much weaker than sub-cloud aerosols, the entrainment of above cloud aerosols may affect the cloud droplets nucleation, and hence change cloud properties near the cloud top to some extent.

## 4 Summary

335 By using in situ aircraft data collected by CIRPAS Twin Otter aircraft at Point Alpha during VOCALS-REx from 16 October to 13 November 2008, we investigated the interaction between aerosol and marine stratocumulus over the southeast Pacific Ocean, especially the dispersion effect. We also explored the entrainment process near the top of stratocumulus and its impacts on cloud properties and aerosol-cloud interaction.

340 Vertical profiles of aerosol, cloud and meteorological variables presented that the BL is well mixed and capped by a sharp inversion during 16 non-drizzling flights. Cloud variables, such as  $LWC$ ,  $N_d$ , and cloud depth, are all positively correlated with sub-cloud CCN number concentration, having the correlation coefficients of 0.60, 0.79 and 0.71, respectively. No evident correlation was found between cloud properties with above-cloud CCN number concentrations. This is mainly due to low aerosol number concentrations above-cloud ( $129.8 \pm 60.1 \text{ cm}^{-3}$ ) and the extremely strong inversion capped the cloud top, which inhibits the mixing of the above-cloud aerosol with cloud layer. Therefore, the influence of above-cloud CCN on cloud 345 properties is very weak compared to sub-cloud CCN. Additionally, the comparison of cloud formation under different aerosol number concentrations conditions suggested that the increase of  $LWC$  is probably ~~controlled~~ contributed by  $N_d$  instead of  $R_e$  in the polluted case due to abundant CCN, in which more but smaller cloud droplets form, while the opposite is true in the clean case.

350 The results showed that both dynamical condition and aerosol microphysical properties have significant effects on cloud droplet formation. In the case of large vertical velocity and aerosol size, the proportion of cloud droplet of total in-cloud particles is relatively high (e.g.  $0.84 \pm 0.12$  and  $0.76 \pm 0.13$ , respectively), i.e., cloud droplets are easier to form. Although chemical components of aerosol is also critical to cloud droplet formation (Nenes et al., 2002; Lance et al., 2004; Ervens et al., 2005; McFiggans et al., 2006; Wang et al., 2008; Almeida et al., 2014), this was not discussed in this study due to unavailable measurements.

355 The correlations between  $\varepsilon$  and  $N_d$  based on the in-flight data, used to represent  $w$ -induced correlation, is significantly negative, while the correlations derived from flight-averaged data (i.e., aerosol-induced correlation) is positive. This implies that an increase in aerosol concentration tends to increase  $\varepsilon$  and  $N_d$  at the same time, while an increase in  $w$  often increases  $N_d$  but decreases  $\varepsilon$ , which is in agreement with theoretical analysis (Liu et al., 2006). After constraining the differences of cloud dynamics between flights, positive correlation between  $\varepsilon$  and  $N_d$  become stronger, indicating that perturbations of  $w$  could 360 weaken the influence of aerosol on  $\varepsilon$ , and hence may result in an underestimation of aerosol dispersion effect. Thus, it requires more attention to isolate the response of relative dispersion to aerosol perturbations from dynamical effects when investigating aerosol dispersion effect and estimating aerosol indirect forcing.

The entrainment in stratocumulus is overall quite weak, and close to adiabatic in some case. In this study, the difference of cloud microphysics between entrainment and non-entrainment zone indicated that the entrainment in stratocumulus is

365 mostly dominated by extreme inhomogeneous entrainment-mixing mechanism. On average, the entrainment reduced  $N_d$  and  $LWC$  by 28.9 % and 24.8 %, respectively, while had little effect on  $D_e$  (only increases by 1.8 %). During flights on Oct. 18, Nov. 04, Nov. 09 and Nov. 13, the entrainment is relatively strong and dilutes  $N_d$  and  $LWC$  by about 50 %. In entrainment zone, the ~~smaller aerosols and~~ drier air entrained from the top result in the smaller  $N_d / (N_d + N_i)$  ( $0.56 \pm 0.22$ ) than that in non-entrainment zone ( $0.73 \pm 0.13$ ). This implies that entrainment may significantly influence cloud droplet formation and hence cloud properties near the top by ~~both inhibiting aerosol activation and~~ promoting cloud droplets evaporation. Furthermore, we also found that the relative dispersion in entrainment zone is larger than that in non-entrainment zone. In addition to the dry and warm air, aerosols with smaller size are also entrained into entrainment zone, but due to the negligible droplet nucleation near the top of stratocumulus, these aerosols seem unlikely to influence cloud droplet formation by inhibiting activation. That is, the effect of entrainment mixing on stratocumulus is mainly determined by the entrained dry air instead of aerosols with different properties from those near the cloud base. But for cumulus, things may be different. Slawinska et al. (2012) found that, in a shallow cumulus, a significant part (40%) of aerosols is activated above cloud base (secondary activation), which is dominated by entrained aerosols. By using large-eddy simulations (LES), Hoffmann et al. (2015) suggested that sub-cloud aerosols and laterally entrained aerosols contribute to all activated aerosols inside the cloud by fractions of 70% and 30%, respectively. Thus, it might be an interesting topic that how and to what extent the entrained aerosols with different properties from sub-cloud aerosols can affect the formation and evolution of clouds. As stated above, although entrainment in stratocumulus is much weaker than that in other cloud types, e.g., cumulus (Warner, 1955, 1969a, 1969b; Blyth et al., 1988; Gerber et al., 2008; Burnet and Brenguier, 2007; Haman et al., 2007), entrainment in strato-cumulus still impact cloud droplet formation near cloud top significantly by entraining ambient dry air as well aerosols with physical and chemical properties different from that in cloud. Therefore, entrainment is important to take into account in studying aerosol-cloud interaction, even in stratocumulus with relatively weak entrainment. However, a quantitative contribution of entrained dry air and aerosols to cloud droplet formation, is difficult to determine only using pure aircraft measurements.

370  
375  
380  
385

*Data availability.* The aircraft measurements data during VOCALS-REx was obtained from the public ftp at [http://data.eol.ucar.edu/master\\_list/?project=VOCALS](http://data.eol.ucar.edu/master_list/?project=VOCALS).

*Competing interests.* The authors declare that they have no conflict of interest.

390 *Acknowledgements.* We are grateful for the dedicated efforts of several support staff and scientists in making the observations from the CIRPAS Twin Otter during VOCALS-REx. We also thank Prof. Bruce Albrecht in University of Miami for kindly providing the aerosol, cloud and meteorological variables observations, which are the basis of this manuscript. This study is supported by the National Natural Science Foundation of China grants (41475005 and 41675004).

## References

- 395 Albrecht, B. A.: Aerosols, cloud microphysics, and fractional cloudiness, *Science*, 245, 1227–1230, 1989.
- Allen, G., Coe, H., Clarke, A. D., Bretherton, C., Wood, R., Abel, S. J., Barrett, P., Brown, P., George, R., Freitag, S., McNaughton, C., Howell, S., Shank, L., Kapustin, V., Brekhovskikh, V., Kleinman, L., Lee, Y.-N., Springston, S., Toniazzo, T., Krejci, R., Fochesatto, J., Shaw, G., Krecl, P., Brooks, B., McMeeking, G., Bower, K. N., Williams, P. I., Crosier, J., Crawford, I., Connolly, P., Allan, J. D., Covert, D., Bandy, A. R., Russell, L. M., Trembath, J., Bart, M.,  
400 McQuaid, J. B., Wang, J., and Chand, D.: South East Pacific atmospheric composition and variability sampled along 20° S during VOCALS-REx, *Atmos. Chem. Phys.*, 11, 5237–5262, 2011.
- Almeida, G. P., Brito, J., Morales, C. A., Andrade, M. F., and Artaxo, P.: Measured and modelled cloud condensation nuclei (CCN) concentration in São Paulo, Brazil: the importance of aerosol size-resolved chemical composition on CCN concentration prediction, *Atmos. Chem. Phys.*, 14, 7559–7572, 2014.
- 405 Andersen, H. and Cermak, J.: How thermodynamic environments control stratocumulus microphysics and interactions with aerosols, *Environ. Res. Lett.*, 10, 24004, 2015.
- Andrejczuk, M., Grabowski, W. W., Malinowski, S. P., and Smolarkiewicz, P. K.: Numerical simulation of cloud-clear air interfacial mixing: Homogeneous versus inhomogeneous mixing, *J. Atmos. Sci.*, 66, 2493–2500, 2009
- Betts, A. K.: Non-precipitating cumulus convection and its parameterization, *Quart. J. R. Met. Soc.*, 99, 178–196, 1973.
- 410 Blyth, A. M., Cooper, W. A., and Jensen, J. B.: A Study of the Source of Entrained Air in Montana Cumuli, *J. Atmos. Sci.*, 45, 3944–3964, 1988.
- Bretherton, C. S., Uttal, T., Fairall, C. W., Yuter, S. E., Weller, R. A., Baumgardner, D., Comstock, K., Wood, R., and Raga, G. B.: The Epic 2001 Stratocumulus Study, *B. Am. Meteorol. Soc.*, 85, 967–977, 2004
- Bretherton, C. S., Wood, R., George, R. C., Leon, D., Allen, G., and Zheng, X.: Southeast Pacific stratocumulus clouds, precipitation and boundary layer structure sampled along 20° S during VOCALS-Rex, *Atmos. Chem. Phys.*, 10, 10639–  
415 10654, 2010.
- Burnet, F. and Brenguier, J. L.: Observational study of the entrainment-mixing process in warm convective clouds, *J. Atmos. Sci.*, 64, 1995–2011, 2007.
- Cai, Y., Snider, J. R., & Wechsler, P. (2013). Calibration of the passive cavity aerosol spectrometer probe for airborne  
420 determination of the size distribution. *Atmospheric Measurement Techniques*, 6(9), 2349.
- Carslaw, K. S., Lee, L. A., Reddington, C. L., Pringle, K. J., Rap, A., Forster, P. M., Mann, G. W., Spracklen, D. V., Woodhouse, M. T., Regayre, L. A., and Pierce, J. R.: Large contribution of natural aerosols to uncertainty in indirect forcing, *Nature*, 503, 67–71, 2013.
- Chand, D., Hegg, D. A., Wood, R., Shaw, G. E., Wallace, D., and Covert, D. S.: Source attribution of climatically important  
425 aerosol properties measured at Paposo (Chile) during VOCALS, *Atmos. Chem. Phys.*, 10, 10789–10801, 2010.
- Chen, Y. and Penner, J. E.: Uncertainty analysis for estimates of the first indirect aerosol effect, *Atmos. Chem. Phys.*, 5, 2935–2948, 2005.
- Chen, Y.-C., Christensen, M. W., Stephens, G. L., and Seinfeld, J. H.: Satellite-based estimate of global aerosol-cloud radiative forcing by marine warm clouds, *Nat. Geosci.*, 7, 643–646, 2014.
- 430 Chen, Y.-C., Christensen, M. W., Diner, D. J., and Garay, M. J.: Aerosol-cloud interactions in ship tracks using

TerraMODIS/MISR, *J. Geophys. Res.-Atmos.*, 120, 2819–2833, 2015.

Costantino, L. and Bréon, F.-M.: Analysis of aerosol-cloud interaction from multi-sensor satellite observations, *Geophys. Res. Lett.*, 37, L11801, 2010.

Costantino, L. and Bréon, F.-M.: Aerosol indirect effect on warm clouds over South-East Atlantic, from co-located MODIS and CALIPSO observations, *Atmos. Chem. Phys.*, 13, 69–88, 2013.

435 [de Roode, S. R. and Wang, Q.: Do stratocumulus clouds detrain? FIRE I data revisited, \*Bound.-Lay. Meteorol.\*, 122, 479–491, doi:10.1007/s10546-006-9113-1, 2007.](#)

[de Rooy, W. C., Bechtold, P., Fröhlich, K., Hohenegger, C., Jonker, H., Mironov, D., Siebesma, A. P., Teixeira, J., Yano, J. I.: Entrainment and detrainment in cumulus convection: an overview, \*Q. J. Roy. Meteorol. Soc.\*, 139, 1–19, 2013.](#)

440 Dusek, U., Frank, G. P., Hildebrandt, L., Curtius, J., Schneider, J., Walter, S., Chand, D., Drewnick, F., Hings, S., Jung, D., Borrmann, S., and Andreae, M. O.: Size matters more than chemistry for cloud-nucleating ability of aerosol particles, *Science*, 312, 1375–1378, 2006.

Ervens, B., Feingold, G., and Kreidenweis, S. M.: Influence of water-soluble organic carbon on cloud drop number concentration, *J. Geophys. Res.*, 110(D18), 18 211, 2005.

445 Ghan, S. J., Abdul-Razzak, H., Nenes, A., Ming, Y., Liu, X., Ovchinnikov, M., Shipway, B., Mekhidze, N., Xu, J., and Shi, X.: Droplet nucleation: Physically-based parameterizations and comparative evaluation, *J. Adv. Model. Earth Syst.*, 3, M10001, 2011.

[Ghate, V. P., Albrecht, B. A., and Kollias, P.: Vertical velocity structure of nonprecipitating continental boundary layer stratocumulus clouds, \*J. Geophys. Res.\*, 115, D13204, doi:10.1029/2009JD013091, 2010.](#)

450 George, R. C. and Wood, R.: Subseasonal variability of low cloud radiative properties over the southeast Pacific Ocean, *Atmos. Chem. Phys.*, 10, 4047–4063, 2010.

Gerber, H., Arends, B. G., and Ackerman, A. S.: A new microphysics sensor for aircraft use, *Atmos. Res.*, 31, 235–252, 1994.

Gerber, H., Frick, G., Malinowski, S. P., Brenguier J.-L., and Burnet, F.: Holes and entrainment in stratocumulus, *J. Atmos. Sci.*, 62, 443–459, 2005.

455 Gerber, H., Frick, G., Jensen, J. B., and Hudson, J. G.: Entrainment, mixing and microphysics in trade-wind cumulus, *J. Meteorol. Soc. Jpn.*, 86A, 87–106, 2008.

[Gerber, H., Malinowski, S. P., and Jonsson, H.: Evaporative and radiative cooling in POST stratocumulus, \*J. Atmos. Sci.\*, 73, 3877–3884, <https://doi.org/10.1175/Jas-D-16-0023.1>, 2016.](#)

460 Gultepe, I. and Isaac, G.: The relationship between cloud droplet and aerosol number concentrations for climate models, *Int. J. Climatol.*, 16, 941–946, 1996.

Haman, K. E., Malinowski, S. P., Kurowski, M. J., Gerber, H., and Brenguier, J.-L.: Small scale mixing processes at the top of a marine stratocumulus – A case study, *Q. J. Roy. Meteor. Soc.*, 133, 213–226, 2007.

Hartmann, D. L., Ockert-Bell, M. E., and Michelsen, M. L.: The effect of cloud type on Earth's energy balance: Global analysis, *J. Climate*, 5, 1281–1304, 1992.

465 Hawkins, L. N., Russell, L. M., Covert, D. S., Quinn, P. K., and Bates, T. S.: Carboxylic acids, sulfates, and organosulfates in processed continental organic aerosol over the southeast Pacific Ocean during VOCALS-Rex 2008, *J. Geophys. Res.*, 115, D13201, 2010.

Hegg, D. A., Covert, D. S., Jonsson, H. H., and Woods, R. K.: A simple relationship between cloud drop number

concentration and precursor aerosol concentration for the regions of Earth's large marine stratocumulus decks, *Atmos. Chem. Phys.*, 12, 1229–1238, 2012.

470 Hoffmann, F., Raasch, S., and Noh, Y.: Entrainment of aerosols and their activation in a shallow cumulus cloud studied with a coupled LCM–LES approach, *Atmos. Res.*, 156, 43–57, 2015.

Hudson, J. G., Noble, S., and Jha, V.: Stratus cloud supersaturations, *Geophys. Res. Lett.*, 37, 21813, 2010.

Hudson, J. G., Noble, S., and Jha, V.: Cloud droplet spectral width relationship to CCN spectra and vertical velocity, *J. Geophys. Res.*, 117, D11211, 2012.

475 Huneeus, N., Gallardo, L., and Rutllant, J. A.: Offshore transport episodes of anthropogenic sulfur in northern Chile: Potential impact on the stratocumulus cloud deck, *Geophys. Res. Lett.*, 33, L19819, 2006.

IPCC, *Climate Change: The Scientific Basis: contributions of Working Group I to the Third Assessment Report of the IPCC*, edited by: Houghton, J. T., Ding, Y., Griggs, D. J., Noguer, M., van der Linden, P. J., Dai, X., Maskell, K., and Johnson, C. A., Cambridge University Press, New York, 881 pp., 2001.

480 IPCC, *Climate Change: The Physical Science Basis: contribution of Working Group 1 to the Fourth Assessment Report of the IPCC*, edited by: Solomon, S., Qin, D., Manning, M., Chen, Z., Marquis, M., Averyt, K. B., Tignor, M., and Miller, H. L., Cambridge University Press, New York, 996 pp., 2007.

IPCC, *Climate change: The Physical Science Basis: contribution of Working group I to the Fifth Assessment Report of the IPCC*, edited by: Stocker, T. F., Dahe, Q., Plattner, G. K., Tignor, M., Allen, S. K., Boschung, J., Nauels, A., Xia, Y., Bex, V., Midgley, P. M., Cambridge University Press, Cambridge, 1535 pp., 2013.

485 Keil, A. and Haywood, J. M.: Solar radiative forcing by biomass burning aerosol particles during safari 2000: a case study based on measured aerosol and cloud properties, *J. Geophys. Res.*, 108(D13), 2003.

Klein, S. A. and Hartmann, D. L.: The Seasonal Cycle of Low Stratiform Clouds, *J. Climate*, 6, 1587–1606, 1993.

490 Kleinman, L. I., Daum, P. H., Lee, Y.-N., Lewis, E. R., Sedlacek III, A. J., Senum, G. I., Springston, S. R., Wang, J., Hubbe, J., Jayne, J., Min, Q., Yum, S. S., and Allen, G.: Aerosol concentration and size distribution measured below, in, and above cloud from the DOE G-1 during VOCALS-REx, *Atmos. Chem. Phys.*, 12, 207–223, 2012.

Koren, I., Kaufman, Y. J., Rosenfeld, D., Remer, L. A., and Rudich, Y.: Aerosol invigoration and restructuring of Atlantic convective clouds, *Geophys. Res. Lett.*, 32, L14828, 2005.

495 Koren, I., Feingold, G., and Remer, L. A.: The invigoration of deep convective clouds over the Atlantic: aerosol effect, meteorology or retrieval artifact?, *Atmos. Chem. Phys.*, 10, 8855–8872, 2010.

Kumar, V. A., Pandithurai, G., Leena, P. P., Dani, K. K., Murugavel, P., Sonbawne, S. M., Patil, R. D., and Maheskumar, R. S.: Investigation of aerosol indirect effects on monsoon clouds using ground-based measurements over a high-altitude site in Western Ghats, *Atmos. Chem. Phys.*, 16(13), 8423–8430, 2016.

500 Lance, S., Nenes, A., and Rissman, T. A.: Chemical and dynamical effects on cloud droplet number: Implications for estimates of the aerosol indirect effect, *J. Geophys. Res.*, 109, 2004.

Lehmann, K., Siebert, H., and Shaw, R. A.: Homogeneous and Inhomogeneous Mixing in Cumulus Clouds: Dependence on Local Turbulence Structure, *J. Atmos. Sci.* 66, 3641–3659, 2009.

Leck, C. and Svensson, E.: Importance of aerosol composition and mixing state for cloud droplet activation over the Arctic pack ice in summer, *Atmos. Chem. Phys.*, 15, 2545–2568, 2015.

505 Lee, Y. N., Springston, S., Jayne, J., Wang, J., Hubbe, J., Senum, G., Kleinman, L., and Daum, P. H.: Chemical composition

and sources of coastal marine aerosol particles during the 2008 VOCALS-REx campaign, *Atmos. Chem. Phys.*, 14, 5057–5072, 2014.

Li, W., Li, P., Sun, G., Zhou, S., Yuan, Q., and Wang, W.: Cloud residues and interstitial aerosols from non-precipitating clouds over an industrial and urban area in northern China, *Atmos. Environ.*, 45, 2488–2495, 2011.

Liu, Y., Leeuw, G. D., Kerminen, V. M., Zhang, J., Zhou, P., Nie, W., Qi, X., Hong, J., Wang, Y., Ding, A., Guo, H., Krüger, O., Kulmala, M., and Petäjä, T.: Analysis of aerosol effects on warm clouds over the Yangtze River Delta from multi-sensor satellite observations, *Atmos. Chem. Phys.*, 17, 5623–5641, 2017.

Liu, Y. G. and Daum, P. H.: Anthropogenic aerosols – Indirect warming effect from dispersion forcing, *Nature*, 419, 580–581, 2002.

Lohmann, U. and Feichter, J.: Global indirect aerosol effects: a review, *Atmos. Chem. Phys.*, 5, 715–737, 2005.

Lu, C., Liu, Y., and Niu, S.: Examination of turbulent entrainment-mixing mechanisms using a combined approach, *J. Geophys. Res.*, 116, D20207, 2011.

Lu, C., Liu, Y., Niu, S., and Vogelmann, A. M.: Observed impacts of vertical velocity on cloud microphysics and implications for aerosol indirect effects, *Geophys. Res. Lett.*, 39, L21808, 2012.

Lu, M.-L., Conant, W. C., Jonsson, H. H., Varutbangkul, V., Flagan, R. C., and Seinfeld, J. H.: The Marine Stratus/Stratocumulus Experiment (MASE): Aerosol-cloud relationships in marine stratocumulus, *J. Geophys. Res.*, 112, D10209, 2007.

Lu, M.-L., Sorooshian, A., Jonsson, H. H., Feingold, G., Flagan, R. C., and Seinfeld, J. H.: Marine stratocumulus aerosol-cloud relationships in the MASE-II experiment: Precipitation susceptibility in eastern Pacific marine stratocumulus, *J. Geophys. Res.*, 114, D24203, 2009.

Ma, J., Chen, Y., Wang, W., Yan, P., Liu, H., Yang, S., Hu, Z., and Lelieveld, J.: Strong air pollution causes widespread haze-clouds over China, *J. Geophys. Res.*, 115, D18204, 2010.

Ma, X., Yu, F., and Quaas, J.: Reassessment of satellite-based estimate of aerosol climate forcing, *J. Geophys. Res.-Atmos.*, 119, 10394–10409, 2014.

Ma, X., Jia, H., Yu, F., and Quaas, J.: Opposite aerosol index-cloud droplet effective radius correlations over major industrial regions and their adjacent oceans, *Geophys. Res. Lett.*, 45, 5771–5778, 2018.

Malinowski, S. P., Gerber, H., Jen-La Plante, I., Kopec, M. K., Kumala, W., Nurowska, K., Chuang, P. Y., Khelif, D., and Haman, K. E.: Physics of Stratocumulus Top (POST): turbulent mixing across capping inversion, *Atmos. Chem. Phys.*, 13, 12171–12186, <https://doi.org/10.5194/acp-13-12171-2013>, 2013.

Martin, G. M., Johnson, D. W., and Spice, A.: The measurement and parameterization of effective radius of droplets in warm stratocumulus clouds, *J. Atmos. Sci.*, 51, 1823–1842, 1994.

McFiggans, G., Artaxo, P., Baltensperger, U., Coe, H., Facchini, M. C., Feingold, G., Fuzzi, S., Gysel, M., Laaksonen, A., Lohmann, U., Mentel, T. F., Murphy, D. M., O’Dowd, C. D., Snider, J. R., and Weingartner, E.: The effect of physical and chemical aerosol properties on warm cloud droplet activation, *Atmos. Chem. Phys.*, 6, 2593–2649, 2006.

McCoy, D. T., Bender, F. M., Mohrmann, J. K. C., Hartmann, D. L., Wood, R., and Grosvenor, D. P.: The global aerosol-cloud first indirect effect estimated using MODIS, MERRA, and AeroCom, *J. Geophys. Res.-Atmos.*, 122, 1779–1796, 2017.

Nenes, A., Charlson, R. J., Facchini, M. C., Kulmala, M., Laaksonen, A., and Seinfeld, J. H.: Can chemical effects on cloud

- 545 droplet number rival the first indirect effect?, *Geophys. Res. Lett.*, 29, 2002.
- [Painemal, D. and Zuidema, P.: Assessment of MODIS cloud effective radius and optical thickness retrievals over the Southeast Pacific with VOCALS-REx in situ measurements, \*J. Geophys. Res.\*, 116, D24206, doi:10.1029/2011jd016155, 2011.](#)
- Pandithurai, G., Dipu, S., Prabha, T. V., Maheskumar, R. S., Kulkarni, J. R., and Goswami, B. N.: Aerosol effect on droplet spectral dispersion in warm continental cumuli, *J. Geophys. Res.*, 117, 2012.
- 550 Pawlowska, H., Brenguier, J. L., and Burnet, F.: Microphysical properties of stratocumulus clouds, *Atmos. Res.*, 55, 15–33, 2000.
- Pawlowska, H., Grabowski, W. W., and Brenguier, J.-L.: Observations of the width of cloud droplet spectra in stratocumulus, *Geophys. Res. Lett.*, 33, L19810, 2006.
- 555 Peng, Y. and Lohmann, U.: Sensitivity study of the spectral dispersion of the cloud droplet size distribution on the indirect aerosol effect, *Geophys. Res. Lett.*, 30, 1507, 2003.
- Peng, Y., Lohmann, U., Leaitch, R., and Kulmala, M.: An investigation into the aerosol dispersion effect through the activation process in marine stratus clouds, *J. Geophys. Res.*, 112, D11117, 2007.
- Pinsky, M. B. and Khain, A. P.: Effects of in-cloud nucleation and turbulence on droplet spectrum formation in cumulus clouds, *Q. J. Roy. Meteor. Soc.*, 128, 501–533, 2002.
- 560 Saponaro, G., Kolmonen, P., Sogacheva, L., Rodriguez, E., Virtanen, T., and de Leeuw, G.: Estimates of the aerosol indirect effect over the Baltic Sea region derived from 12 years of MODIS observations, *Atmos. Chem. Phys.*, 17, 3133–3143, 2017.
- Slawinska, J., Grabowski, W. W., Pawlowska, H., and Morrison, H.: Droplet activation and mixing in large-eddy simulation of a shallow cumulus field, *J. Atmos. Sci.*, 69, 444–462, 2012.
- 565 [Stevens, B.: Entrainment in stratocumulus-topped mixed layers, \*Q. J. Roy. Meteorol. Soc.\*, 128, 2663–2690, doi:10.1256/qj.01.202, 2002](#)
- Su, W., N. G. Loeb, K.-M. Xu, G. L. Schuster, and Z. A. Eitzen: An estimate of aerosol indirect effect from satellite measurements with concurrent meteorological analysis, *J. Geophys. Res.*, 115, D18219, 2010.
- 570 Tang, J., Wang, P., Mickley, L. J., Xia, X., Liao, H., Yue, X., Sun, L., and Xia, J.: Positive relationship between liquid cloud droplet effective radius and aerosol optical depth over Eastern China from satellite data, *Atmos. Environ.*, 84, 244–253, 2014.
- Twohy, C. H., Austin, P. H., and Charlson, R. J.: Chemical consequences of the initial diffusional growth of cloud droplets: a clean marine case, *Tellus B*, 41, 51–60, 1989.
- 575 Twohy, C. H., Anderson, J. R., Toohey, D. W., Andrejczuk, M., Adams, A., Lytle, M., George, R. C., Wood, R., Saide, P., Spak, S., Zuidema, P., and Leon, D.: Impacts of aerosol particles on the microphysical and radiative properties of stratocumulus clouds over the southeast Pacific Ocean, *Atmos. Chem. Phys.*, 13, 2541–2562, 2013.
- Twomey, S.: Pollution and Planetary Albedo, *Atmos. Environ.*, 8, 1251–1256, 1974.
- Wang, F., Guo, J., Wu, Y., Zhang, X., Deng, M., Li, X., Zhang, J., and Zhao, J.: Satellite observed aerosol-induced variability in warm cloud properties under different meteorological conditions over eastern China, *Atmos. Environ.*, 84, 122–132, 580 2014.
- Wang, F., Guo, J., Zhang, J., Huang, J., Min, M., Chen, T., Liu, H., Deng, M., and Li, X.: Multi-sensor quantification of

aerosol-induced variability in warm clouds over eastern China, *Atmos. Environ.*, 113, 1–9, 2015.

585 [Wang, Q. and Albrecht, B. A.: Observations of cloud-top entrainment in marine stratocumulus clouds, \*J. Atmos. Sci.\*, 51, 1530–1547, 1994.](#)

Warner, J.: The water content of cumuliform cloud, *Tellus*, 7, 449–457, 1955.

Warner, J.: The Microstructure of Cumulus Cloud. Part I. General Features of the Droplet Spectrum, *J. Atmos. Sci.*, 26, 1049–1059, 1969a.

590 Warner, J.: The microstructure of cumulus clouds. Part II. The effect on droplet size distribution of cloud nucleus spectrum and updraft velocity, *J. Atmos. Sci.*, 26, 1272–1282, 1969b.

[Wood, R.: Stratocumulus clouds, \*Mon. Weather Rev.\*, 140, 2373–2423, doi:10.1175/MWR-D-11-00121.1, 2012.](#)

Wood, R., Bretherton, C., Huebert, B., Mechoso, C. R., and Weller, R.: VOCALS-SouthEast Pacific Regional Experiment (REx), Scientific program overview, 2006.

595 Wood, R., Comstock, K. K., Bretherton, C. S., Cornish, C., Tomlinson, J., Collins, D. R., and Fairall, C.: Open cellular structure in marine stratocumulus sheets, *J. Geophys. Res.*, 113, D12207, 2008.

Wood, R., Mechoso, C. R., Bretherton, C. S., Weller, R. A., Huebert, B., Straneo, F., Albrecht, B. A., Coe, H., Allen, G., Vaughan, G., Daum, P., Fairall, C., Chand, D., Gallardo Klenner, L., Garreaud, R., Grados, C., Covert, D. S., Bates, T. S., Krejci, R., Russell, L. M., de Szoeke, S., Brewer, A., Yuter, S. E., Springston, S. R., Chaigneau, A., Toniazzo, T., Minnis, P., Palikonda, R., Abel, S. J., Brown, W. O. J., Williams, S., Fochesatto, J., Brioude, J., and Bower, K. N.: The VAMOS Ocean-Cloud-Atmosphere-Land Study Regional Experiment (VOCALS-REx): goals, platforms, and field operations, *Atmos. Chem. Phys.*, 11, 627–654, 2011.

600 Yum, S. S., Wang, J., Liu, Y., Senum, G., Springston, S., McGraw, R., and Yeom, J. M.: Cloud microphysical relationships and their implication on entrainment and mixing mechanism for the stratocumulus clouds measured during the VOCALS project, *J. Geophys. Res.-Atmos.*, 120, 5047–5069, 2015.

Zhao, C., Tie, X., Brasseur, G., Noone, K. J., Nakajima, T., Zhang, Q., Zhang, R., Huang, M., Duan, Y., Li, G., and Ishizaka, Y.: Aircraft measurements of cloud droplet spectral dispersion and implications for indirect aerosol radiative forcing, *Geophys. Res. Lett.*, 33, L16809, 2006.

610 Zhang, Q., Quan, J., Tie, X., Huang, M., and Ma, X.: Impact Aerosol Particles on Cloud Formation: Aircraft Measurements in Beijing, China, *Atmos. Environ.*, 45, 665–672, 2011.

Zheng, X., Albrecht, B. A., Minnis, P., Ayers, K., and Jonson, H. H.: Observed aerosol and liquid water path relationships in marine stratocumulus, *Geophys. Res. Lett.*, 37, L17803, 2010.

615 Zheng, X., Albrecht, B., Jonsson, H. H., Khelif, D., Feingold, G., Minnis, P., Ayers, K., Chuang, P., Donaher, S., Rossiter, D., Ghate, V., Ruiz-Plancarte, J., and Sun-Mack, S.: Observations of the boundary layer, cloud, and aerosol variability in the southeast Pacific near-coastal marine stratocumulus during VOCALSREx, *Atmos. Chem. Phys.*, 11, 9943–9959.

**Table 1. Correlations between  $\varepsilon$  and  $N_d$  ( $N_a$ ) from observation studies.**

Observations	Observation type	Location	Data for correlation analysis	Correlation
Liu and Daum, 2002	Aircraft	Ocean & coast	Flight-averaged	Positive
Peng and Lohmann, 2003	Aircraft	Coast	Flight-averaged	Positive
Pawlowska et al., 2006	Aircraft	Ocean	In-flight Flight-averaged	Negative Positive
Zhao et al., 2006	Aircraft	Land, ocean, and coast	In-flight	$\varepsilon$ converges to a small range of values with increasing $N_d$
Lu et al., 2007	Aircraft	Ocean	In-flight Flight-averaged	Negative None for $N_d$ ; Positive for $N_a$
Lu et al., 2012	Aircraft	Land	In-flight Flight-averaged	Negative Negative
Hudson et al., 2012	Aircraft	Ocean	Flight-averaged	Negative
Ma et al., 2012	Aircraft	Land	Flight-averaged	Negative
Pandithurai et al., 2012	Aircraft	Land	Flight-averaged	Positive
Kumar et al., 2016	ground-based	Land	—	Positive

**Table 2. Flight information and parameters that represent the properties of entrainment during all 16 non-drizzling flights.**

Flight number	RF01	RF02	RF03	RF04	RF05	RF06	RF07	RF08	RF09
Date	10.16	10.18	10.19	10.21	10.22	10.24	10.26	10.27	10.29
BL type	<b>Typical</b>	<b>Typical</b>	<b>Typical</b>	<b>Typical</b>	<b>Typical</b>	<b>Other</b>	<b>Typical</b>	<b>Typical</b>	<b>Other</b>
						Wind shear			Decoupled
<i>w ave</i> <sup>a</sup>	<u>0.09</u>	<u>0.08</u>	<u>0.11</u>	<u>0.08</u>	<u>0.08</u>	<u>-0.06</u>	<u>0.06</u>	<u>0.08</u>	<u>-0.13</u>
<i>w std</i> <sup>b</sup>	<u>0.42</u>	<u>0.55</u>	<u>0.58</u>	<u>0.51</u>	<u>0.51</u>	<u>0.30</u>	<u>0.56</u>	<u>0.41</u>	<u>0.61</u>
<i>w skew</i> <sup>c</sup>	<u>-0.38</u>	<u>-0.16</u>	<u>-0.27</u>	<u>-0.21</u>	<u>-0.27</u>	<u>0.00</u>	<u>-0.23</u>	<u>0.08</u>	<u>-0.27</u>
<i>P<sub>LWC</sub></i> <sup>da</sup>	25.8	55.7	33.4	24.8	24.6	29.3	-2.7	11.2	3.1
<i>P<sub>Nd</sub></i> <sup>db</sup>	32.1	60.1	30.1	38.6	28.2	34.4	4.9	19.6	6.4
<i>P<sub>De</sub></i> <sup>de</sup>	-1.9	-5.7	0.9	-6.7	-1.9	-0.1	-4.1	-2.4	-1.8
<i>AF<sub>ent</sub></i> <sup>gd</sup>	0.77	0.52	0.58	0.85	0.49	0.52	0.51	0.76	0.81
<i>AF<sub>non-ent</sub></i> <sup>he</sup>	0.95	0.84	0.82	0.77	0.74	0.78	0.73	0.82	0.80
Flight Number	RF10	RF11	RF12	RF13	RF14	RF15	RF16	Total	
Date	10.30	11.04	11.08	11.09	11.10	11.12	11.13		
BL type	<b>Other</b>	<b>Other</b>	<b>Other</b>	<b>Typical</b>	<b>Typical</b>	<b>Typical</b>	<b>Other</b>		
	Wind shear	Wind shear,	Decoupled				Wind Shear		
		Decoupled							
<i>w ave</i>	<u>0.02</u>	<u>0.07</u>	<u>0.02</u>	<u>0.08</u>	<u>0.09</u>	<u>0.09</u>	<u>-0.02</u>		
<i>w std</i>	<u>0.45</u>	<u>0.41</u>	<u>0.42</u>	<u>0.47</u>	<u>0.49</u>	<u>0.51</u>	<u>0.41</u>		
<i>w skew</i>	<u>-0.13</u>	<u>-0.48</u>	<u>-0.03</u>	<u>-0.48</u>	<u>-0.26</u>	<u>-0.27</u>	<u>-0.42</u>		
<i>P<sub>LWC</sub></i>	10.5	62.1	2.5	55.8	2.9	-1.8	58.7	24.8	
<i>P<sub>Nd</sub></i>	7.6	56.3	24.0	56.1	-1.6	7.5	59.2	28.9	
<i>P<sub>De</sub></i>	0.2	4.4	-8.4	-2.1	3.4	-2.5	-1.2	-1.8	
<i>AF<sub>ent</sub></i>	0.73	0.66	0.84	0.28	0.70	0.67	0.56	0.64	
<i>AF<sub>non-ent</sub></i>	0.82	0.97	0.77	0.50	0.79	0.60	0.64	0.77	

<sup>a, b, c</sup> *w ave*, *w std*, and *w skew* are the average, standard deviation, and skewness of in-cloud vertical velocities, respectively.

<sup>da, db, de</sup> *P<sub>LWC</sub>*, *P<sub>Nd</sub>*, and *P<sub>De</sub>* are the percentages of reduction in *LWC*, *N<sub>d</sub>* and *D<sub>e</sub>* within entrainment zone relative to non-entrainment zone.(unit: %)

<sup>gd, he</sup> *AF<sub>ent</sub>* and *AF<sub>non-en</sub>* are adiabatic fraction in entrainment zone and non-entrainment zone, respectively. Here, adiabatic fraction is defined as the ratio of the measured to its adiabatic *LWC* that is calculated using pressure and temperature near cloud base.

620

625

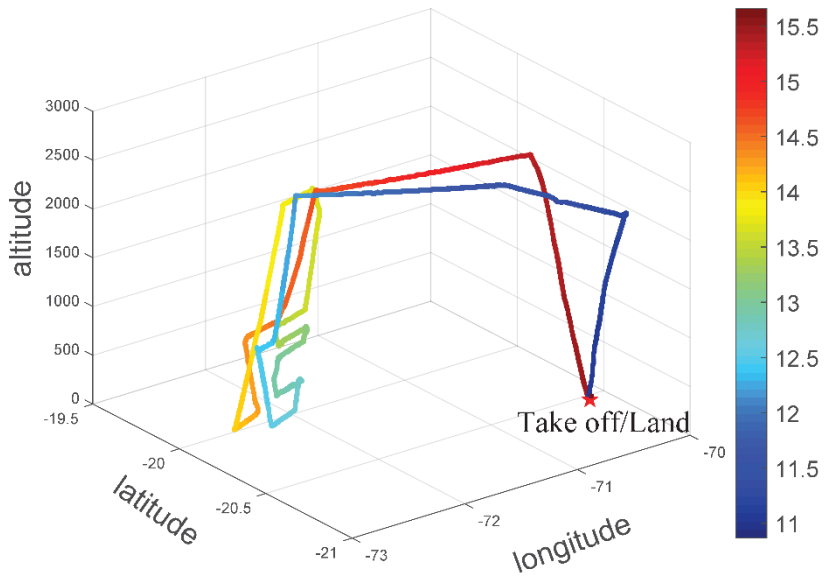
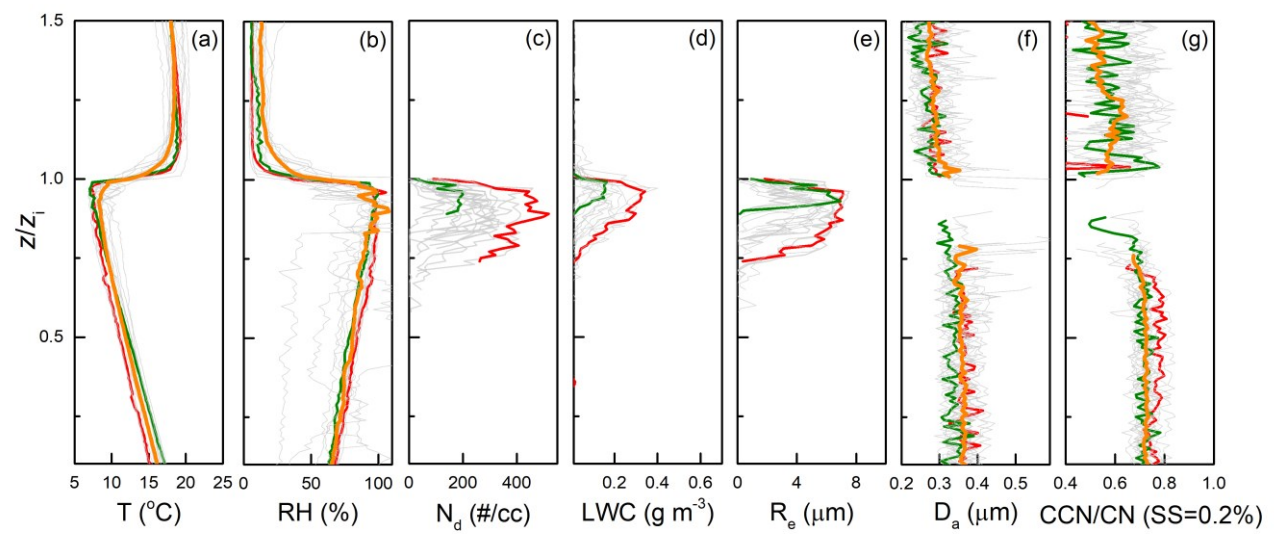
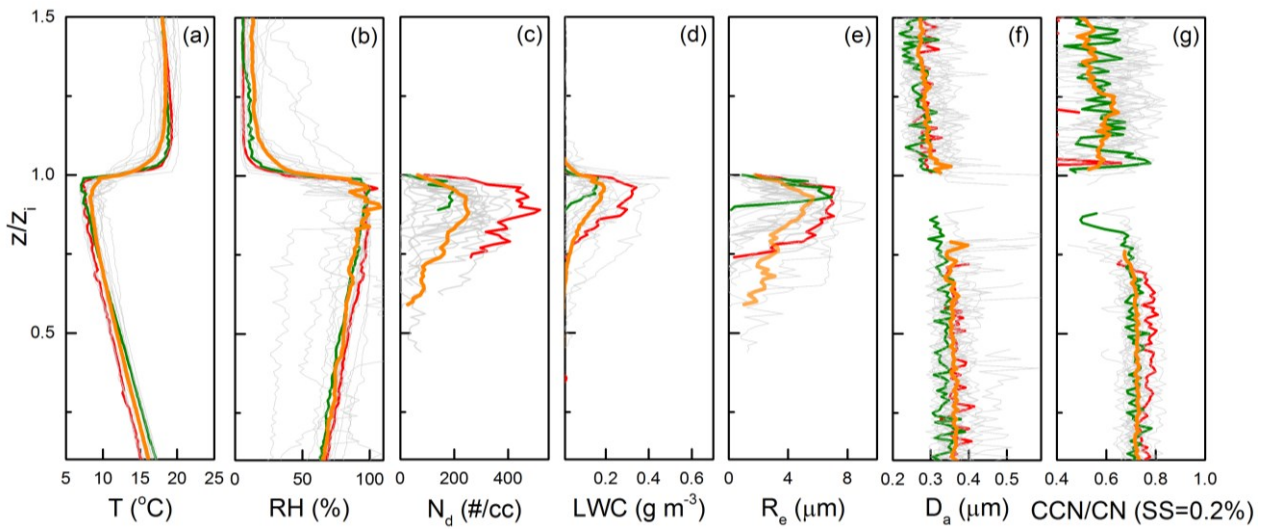


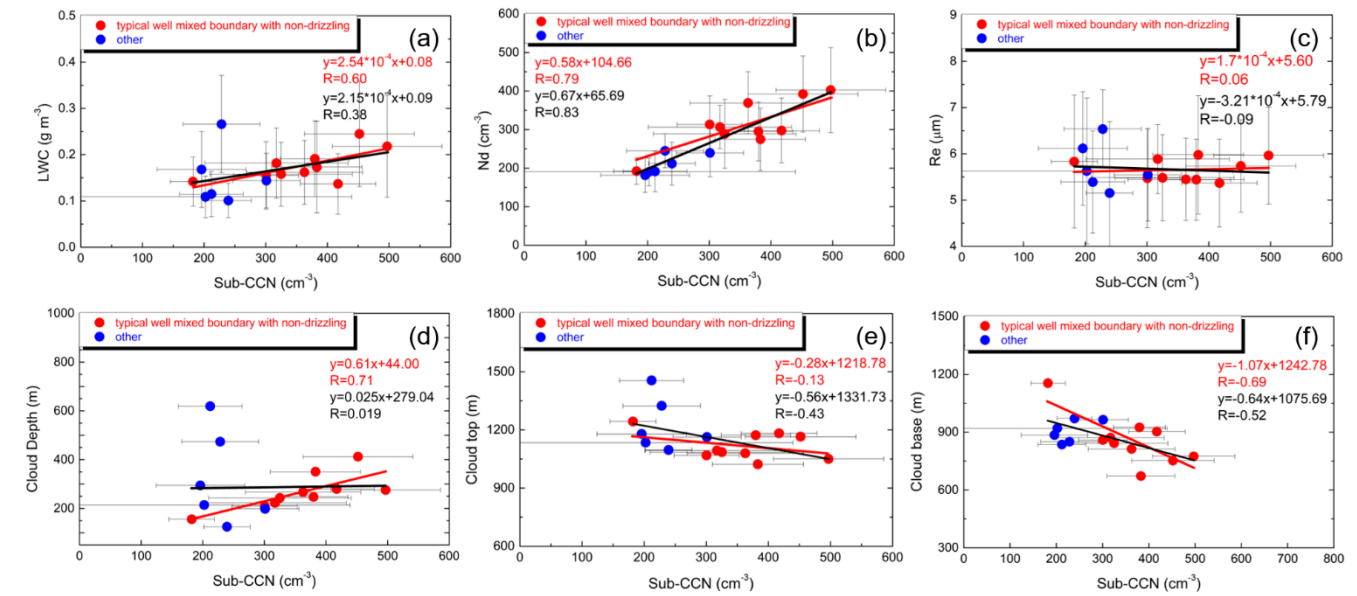
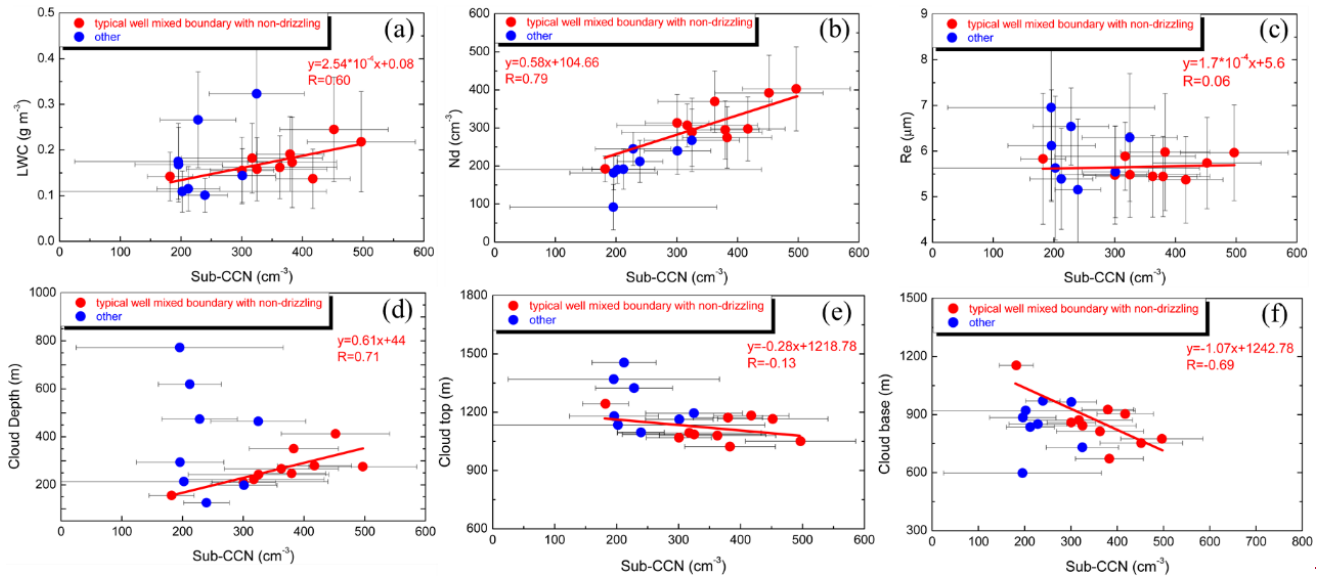
Fig. 1. The flight track in Oct. 18, and the colors represent flight time in hour (UTC).



630

Fig. 2. Vertical profiles scaled by the inversion height. (a) temperature (K); (b) relative humidity (%); (c) cloud droplet number concentration ( $\text{cm}^{-3}$ ); (d) liquid water content ( $\text{g m}^{-3}$ ); (e) effective radius of cloud droplets ( $\mu\text{m}$ ); (f) effective diameter of aerosols ( $\mu\text{m}$ ), and (g) the number concentration ratio of CCN to aerosols for all 16 non-drizzling flights. The gray lines show all individual flights, and the orange lines indicate the average profiles. The red and green lines represent the polluted (Oct. 18) and clean (Nov. 9) cases, respectively.

635



640

Fig. 3. (a)  $LWC$  ( $\text{g cm}^{-3}$ ); (b)  $N_d$  ( $\text{cm}^{-3}$ ); (c)  $R_e$  ( $\mu\text{m}$ ); (d) cloud depth (m); (e) cloud top height (m); (f) cloud base height (m) as a function of sub-cloud CCN concentrations ( $SS=0.2\%$ ) for all 16 non-drizzling flights. The error bars through these symbols indicate the standard deviation. Red symbols are the typical well mixed boundary with non-drizzling discussed in Zheng et al. (2011), and

blue symbols for others. Red (black) texts are the correlation coefficient for typical well mixed cases (all cases).

645

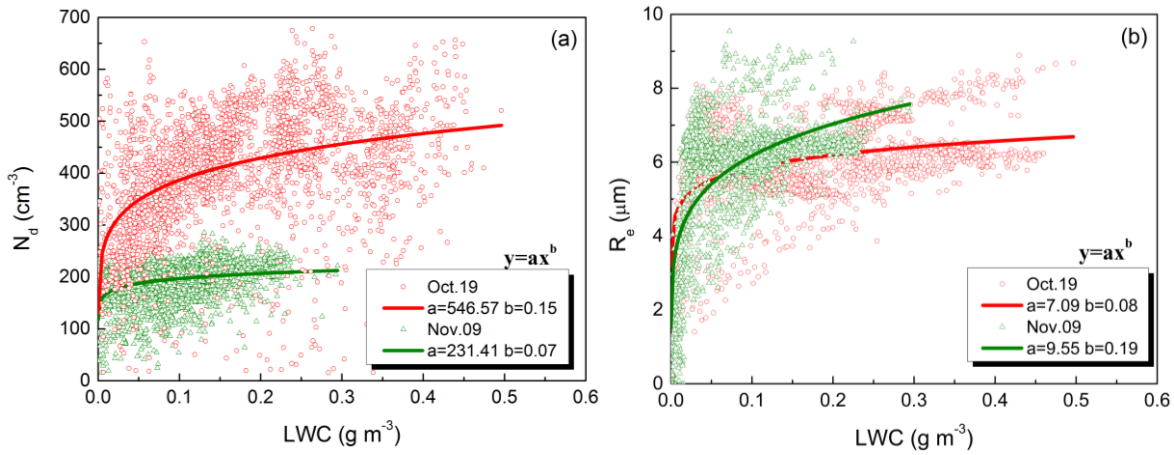


Fig. 4. Correlations between (a)  $N_d$  ( $\text{cm}^{-3}$ ), (b)  $R_e$  ( $\mu\text{m}$ ) and  $LWC$  ( $\text{g m}^{-3}$ ) for clean (green) and polluted (red) cases, respectively.

650

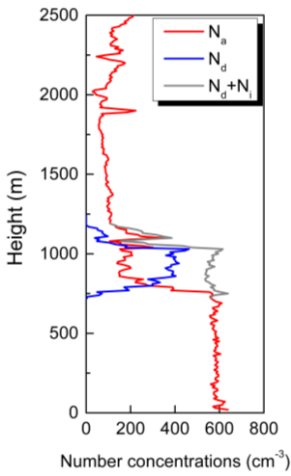


Fig. 5. Vertical profiles of number concentrations of aerosols ( $N_a$ ), cloud droplets ( $N_d$ ) and total in-cloud particles ( $N_d + N_i$ ) during the flight on Oct. 18.

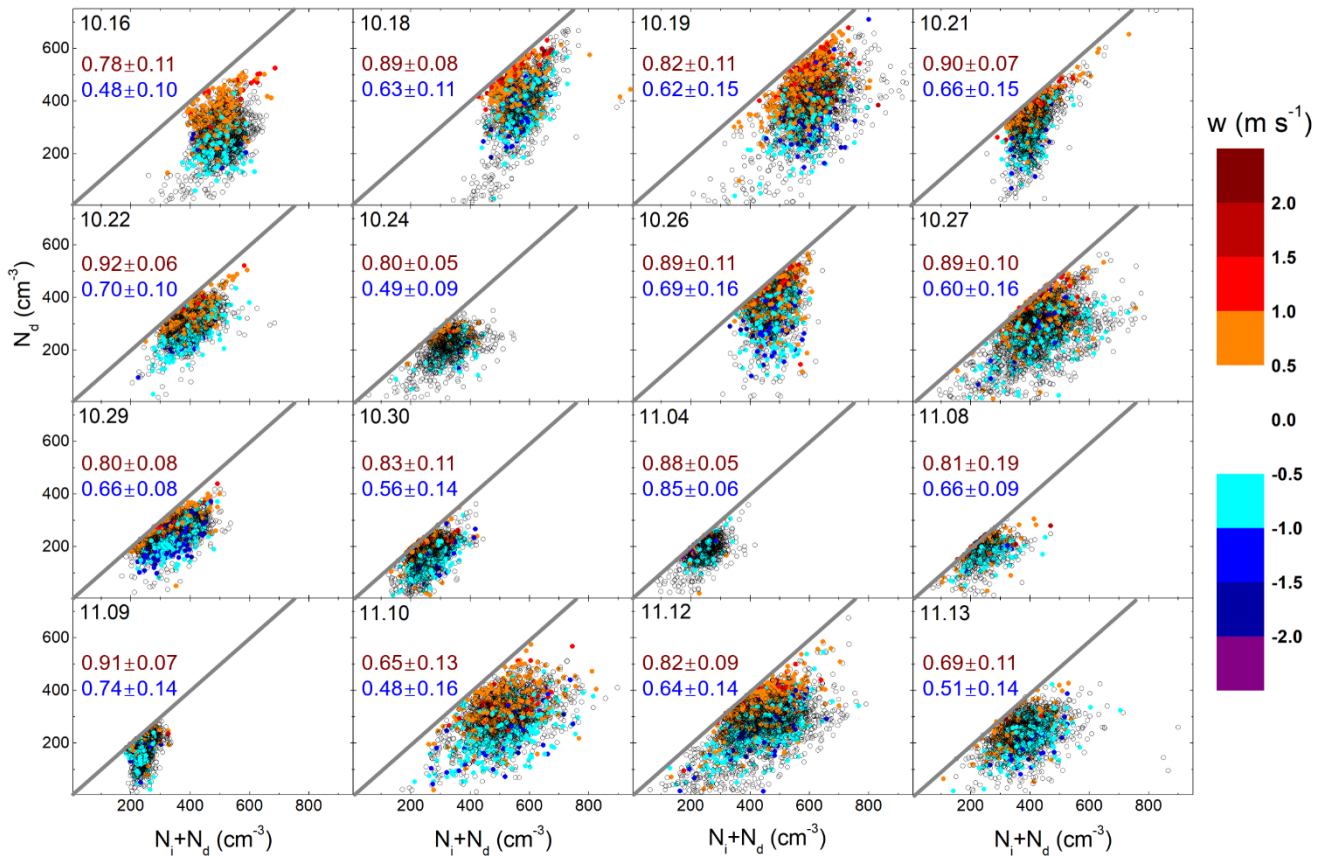
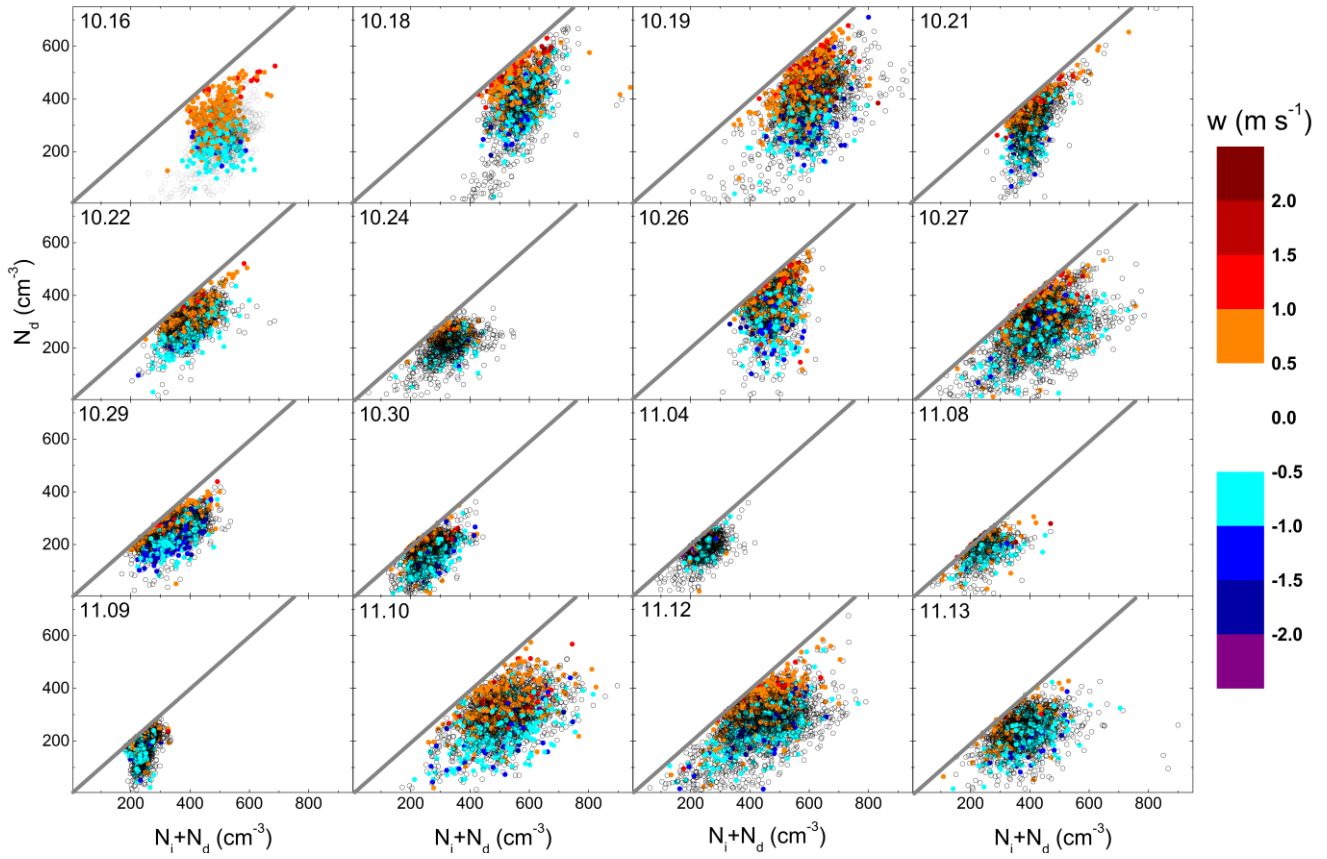


Fig. 6. Relationships between  $N_d$  and  $N_i + N_d$  during all 16 non-drizzling flights. The colors represent in-cloud vertical velocities ( $\text{m s}^{-1}$ ), and gray line is 1:1 line. **The mean and standard deviation of  $N_d/(N_d + N_i)$  for vertical velocity greater than  $1 \text{ m s}^{-1}$  (red) and less**

than  $-1 \text{ m s}^{-1}$  (blue) are shown.

660

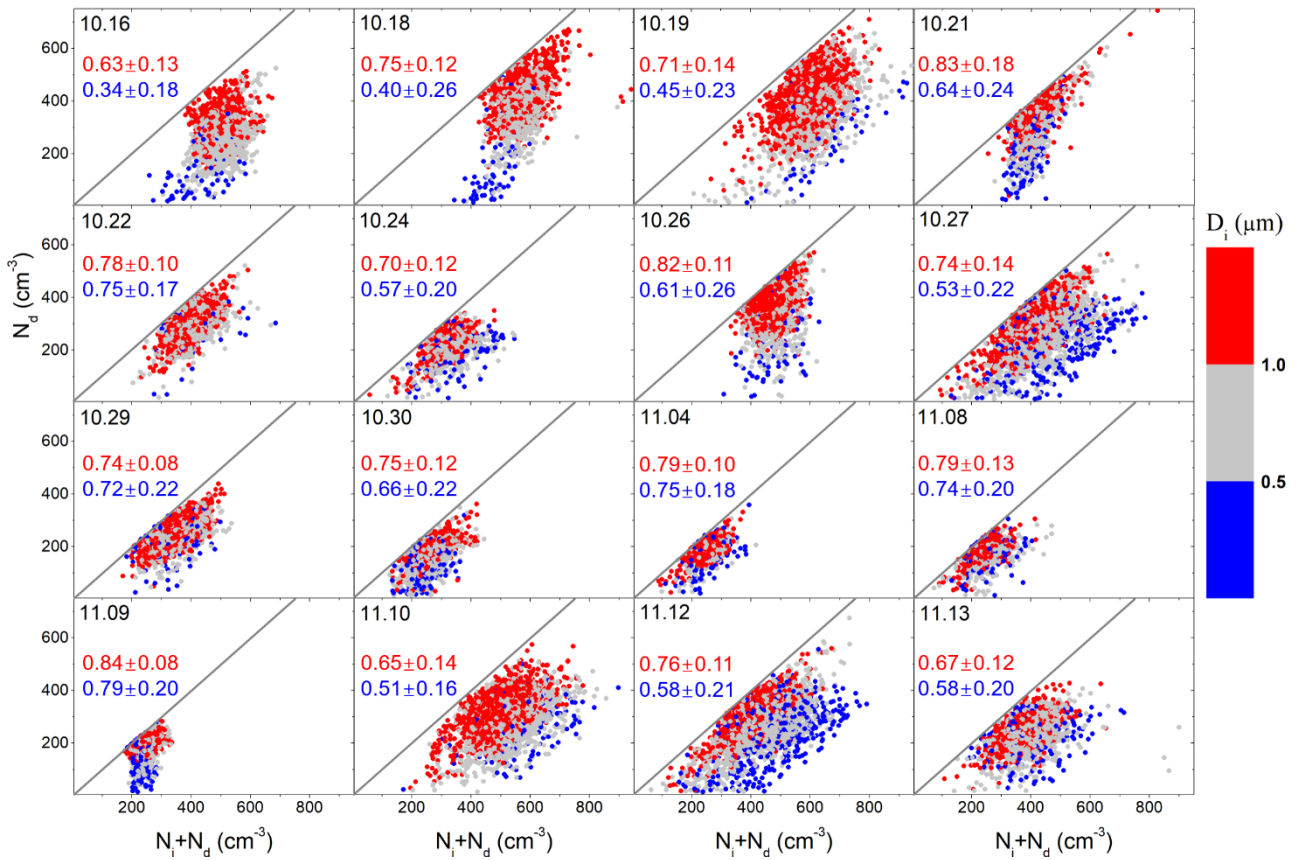
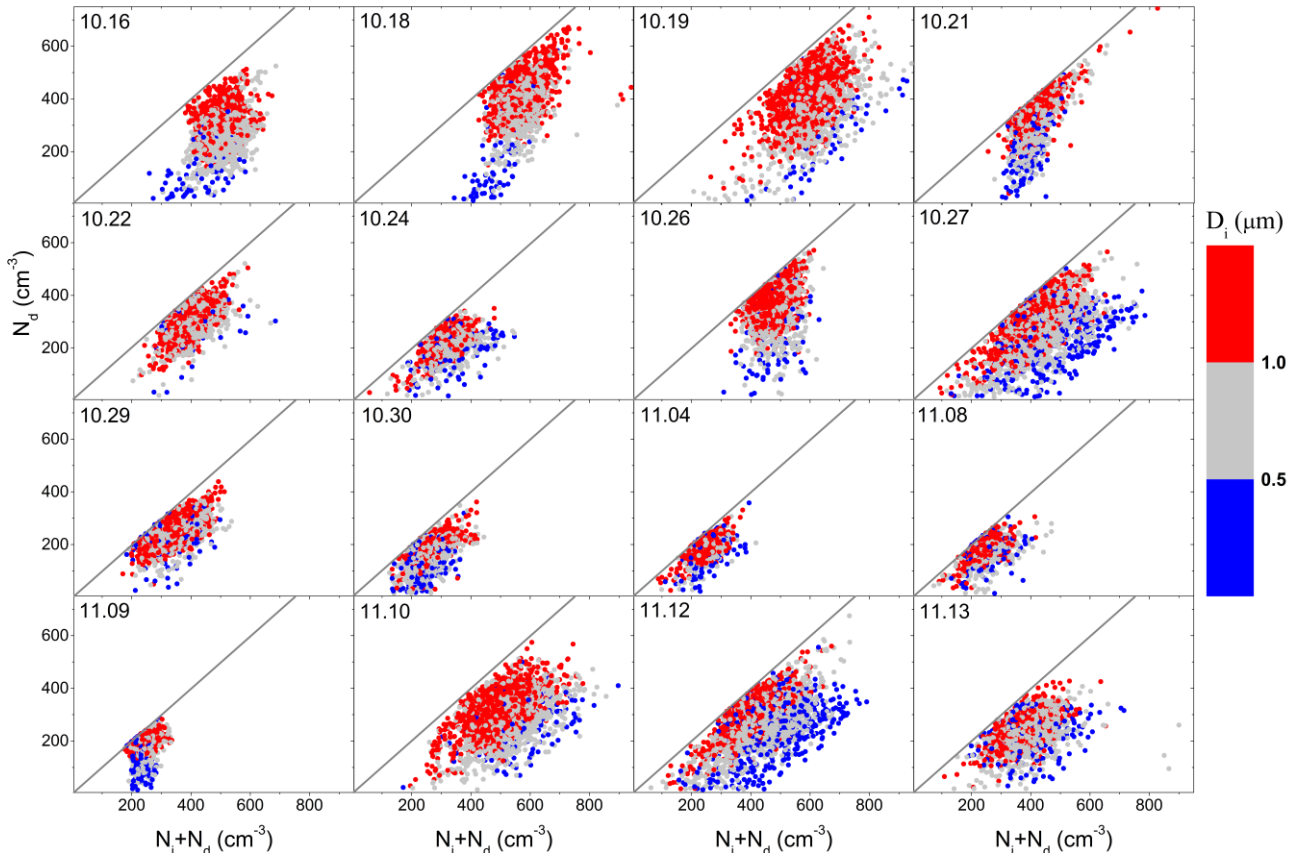
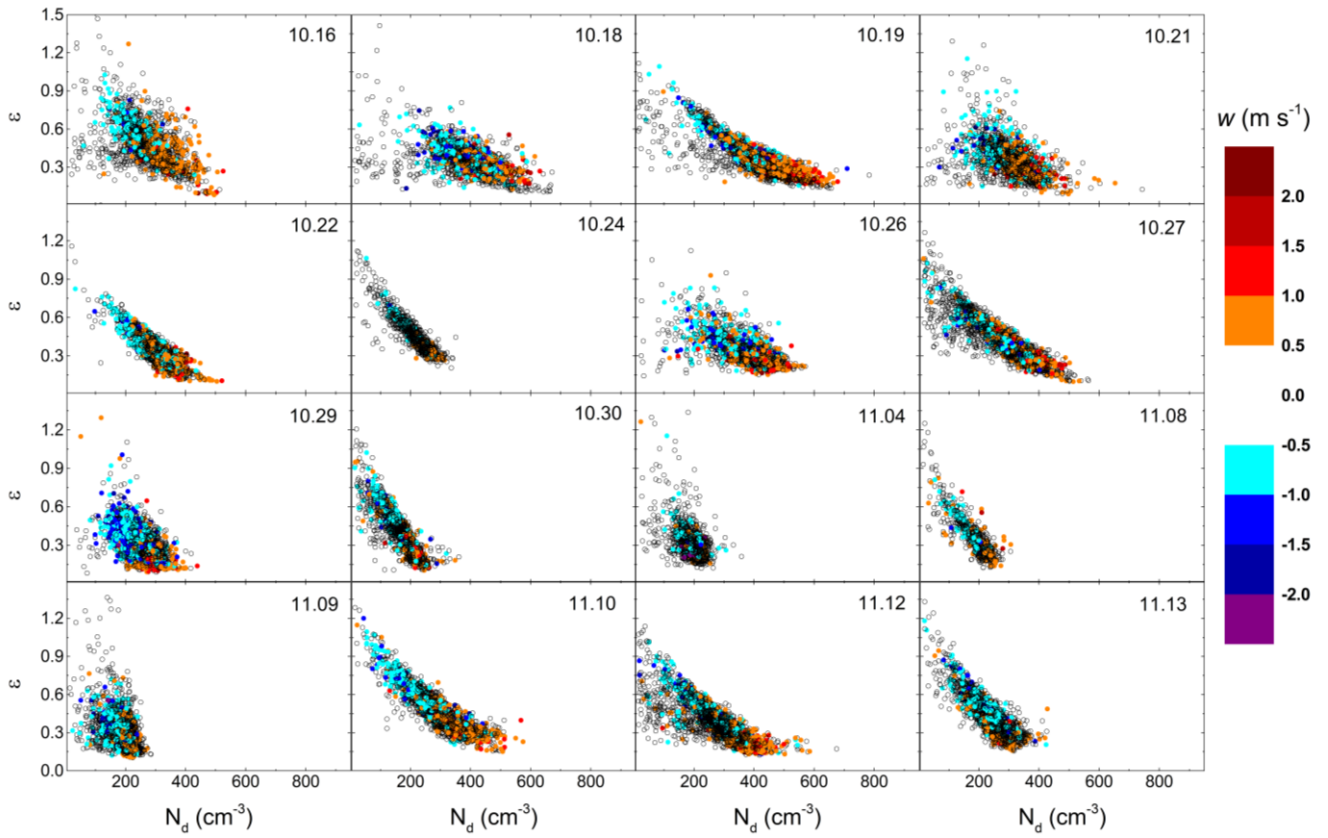
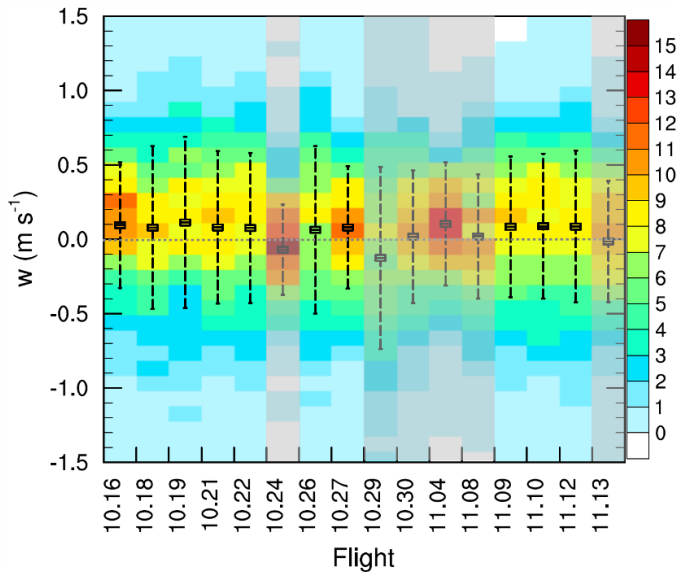


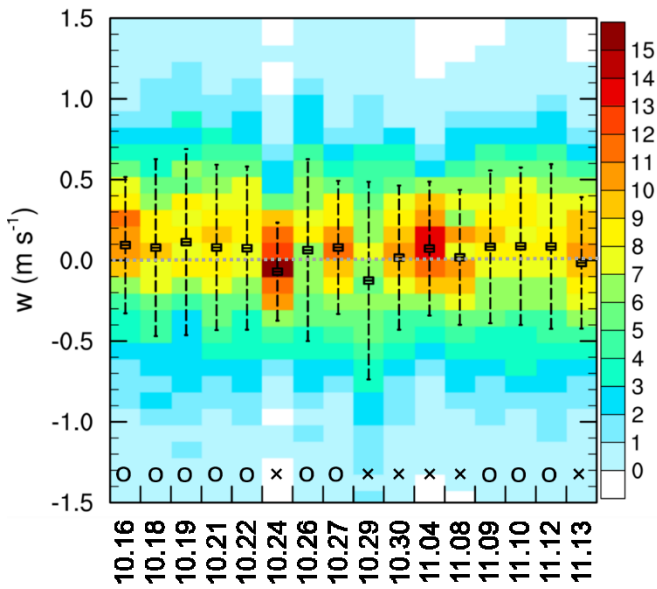
Fig. 7. Same as Fig. 6, but the colors represent the effective diameter of interstitial aerosol ( $D_i$ ) ( $\mu\text{m}$ ). The mean and standard deviation of  $N_d/(N_d+N_i)$  for  $D_i$  greater than  $1 \mu\text{m}$  (red) and less than  $0.5 \mu\text{m}$  (blue) are shown.



665

**Fig. 8.** Relationships between relative dispersion ( $\epsilon$ ) and  $N_d$  during all 16 non-drizzling flights, in which the colors representing in-cloud vertical velocities ( $\text{m s}^{-1}$ ).





670

Fig. 9. Probability distribution function (units: %) of vertical velocity ( $w$ ) for 16 non-drizzling flights. Black symbols are mean values of  $w$ , and error bars through these symbols indicate the standard deviation. ~~Gray shadow represents the flights other than typical well-mixed boundary with non-drizzling.~~ Circles are the typical well mixed boundary with non-drizzling, and crosses for others.

675

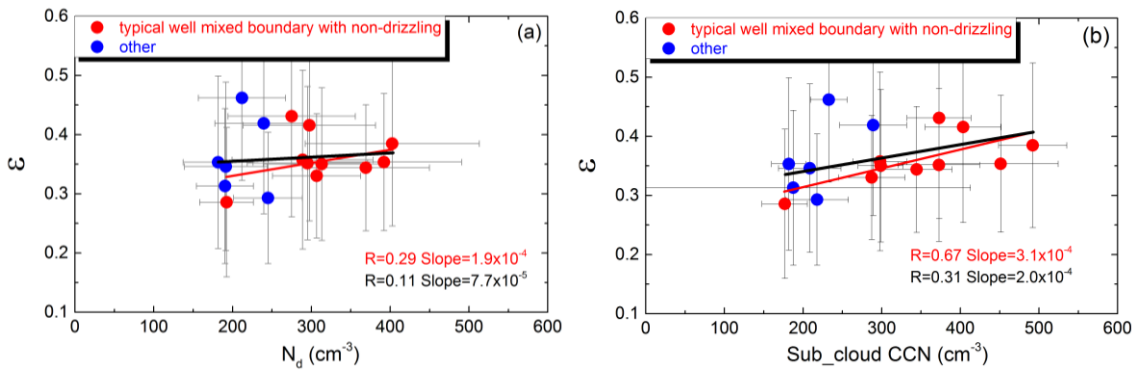


Fig. 10. Relative dispersion ( $\epsilon$ ) as a function of (a)  $N_d$  and (b) sub-cloud CCN concentrations ( $SS=0.2\%$ ) for all flights. The error bars through these symbols indicate the standard deviation. Red symbols are the typical well mixed boundary with non-drizzling, and blue symbols for others. Red (black) texts are the correlation coefficient and slope for typical well mixed cases (all cases).

680

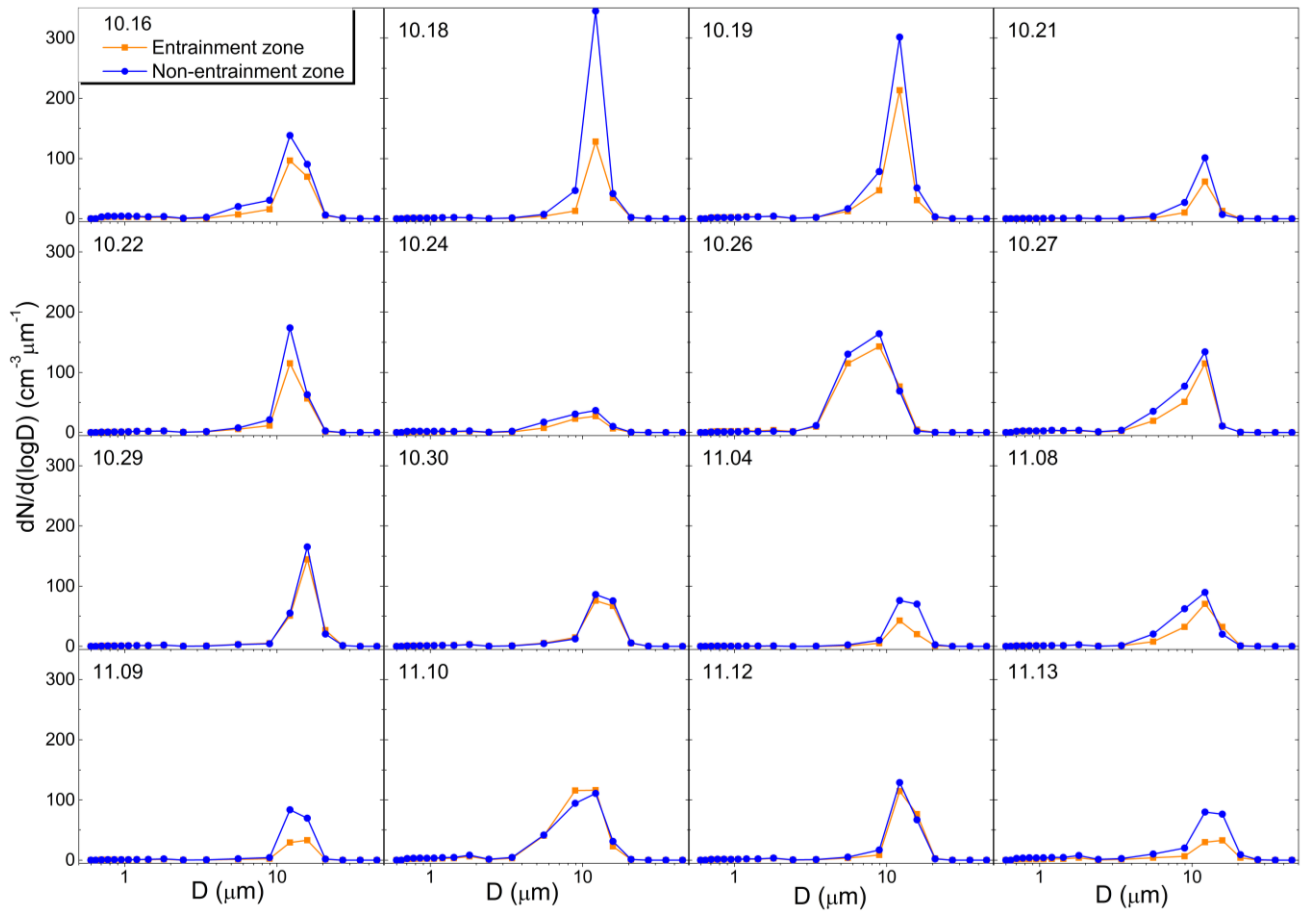


Fig. 11. Number size distributions of cloud droplets in entrainment (yellow) and non-entrainment zone (blue) during all 16 non-drizzling flights.

685

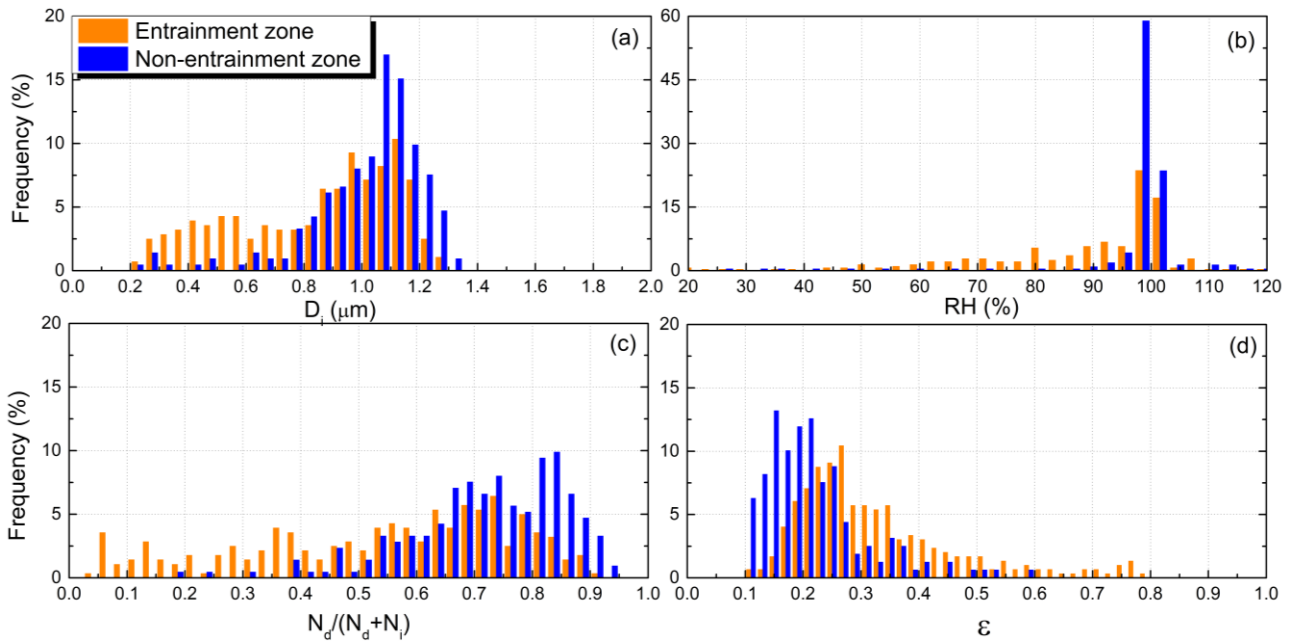


Fig. 12. Probability density functions of (a)  $D_i$  ( $\mu\text{m}$ ), (b)  $RH$  (%), (c)  $N_d/(N_d + N_i)$ , and (d)  $\varepsilon$  in entrainment (yellow) and non-entrainment zone (blue) during the flight on Oct. 18.

*Supplement of*

**Exploring aerosol cloud interaction using VOCALS-REx  
aircraft measurements**

Hailing Jia, Xiaoyan Ma and Yangang Liu

*Correspondence to:* Xiaoyan Ma (xma@nuist.edu.cn)

### Figure List

Figure S1. Normalized profiles of  $N_d$ . Values of  $Z_N=0$  indicates the cloud base whereas  $Z_N=1$  the cloud top. Orange line indicates the average profiles.

Figure S2. (a)  $P_{LWC}$  and (b)  $P_{N_d}$  as a function of  $AF_{ent}/AF_{non-ent}$  for all 16 non-drizzling flights.

**Figure S1**

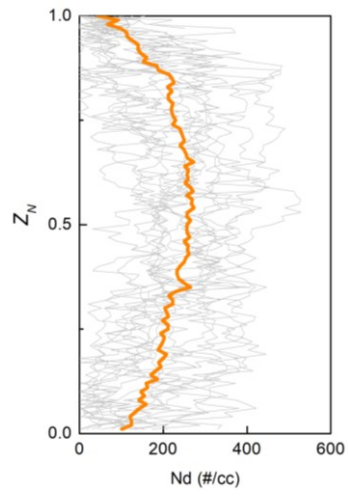


**Figure S2**

